SEISMIC CYCLE

- Elastic accumulation and rupture on a fault. Exemple on a Strike-slip fault and a Subduction fault
- Size of an earthquake
- Time dependent station motion and earthquake cycle : READ and Wallace models
- Pre-seismic, co-seismic and post-seismic motions
- Clustering and Triggering of earthquake (Coulomb stress interractions)
- Precursors ?

Arctang profiles

$$U_y = 2 \cdot {}^{V_0}/_{\Pi} \text{ arctang } ({}^{x}/_{h})$$

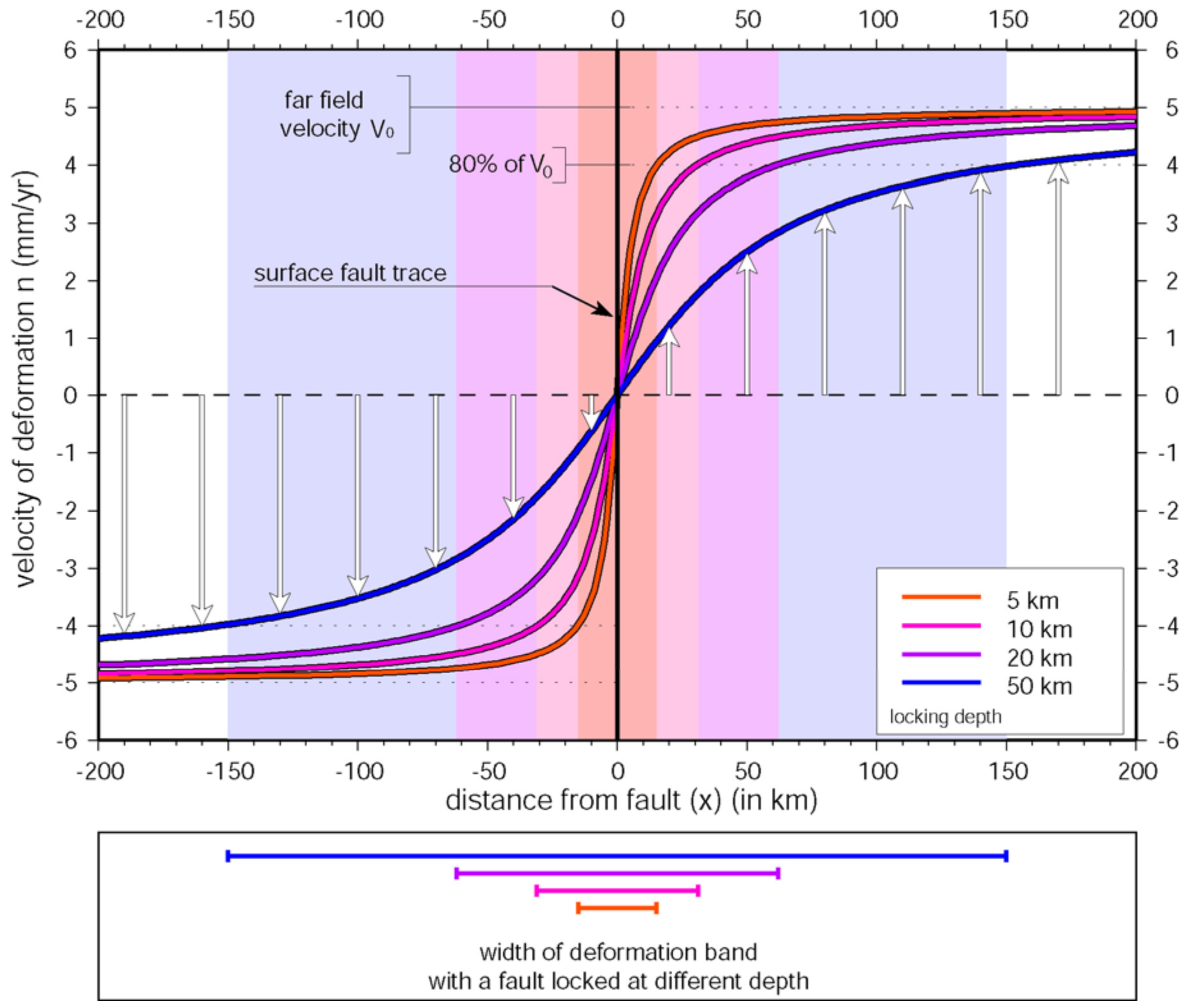

Elastic accumulation and rupture

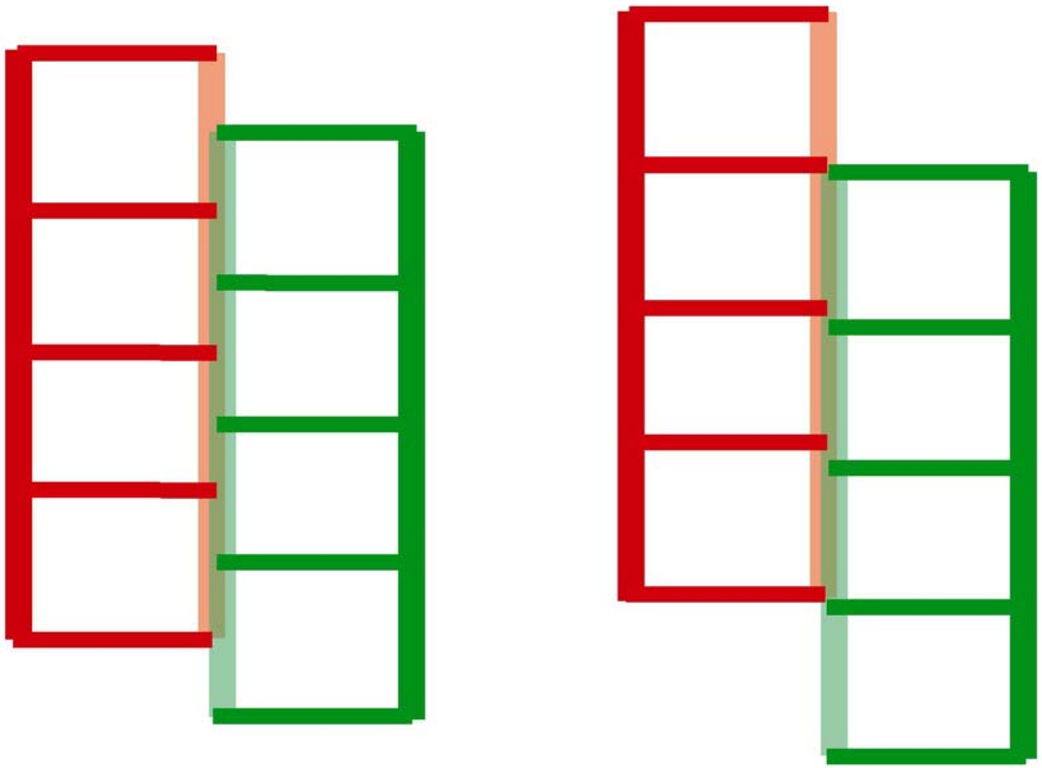

earthquake earthquake

Seismic cycle in subduction context

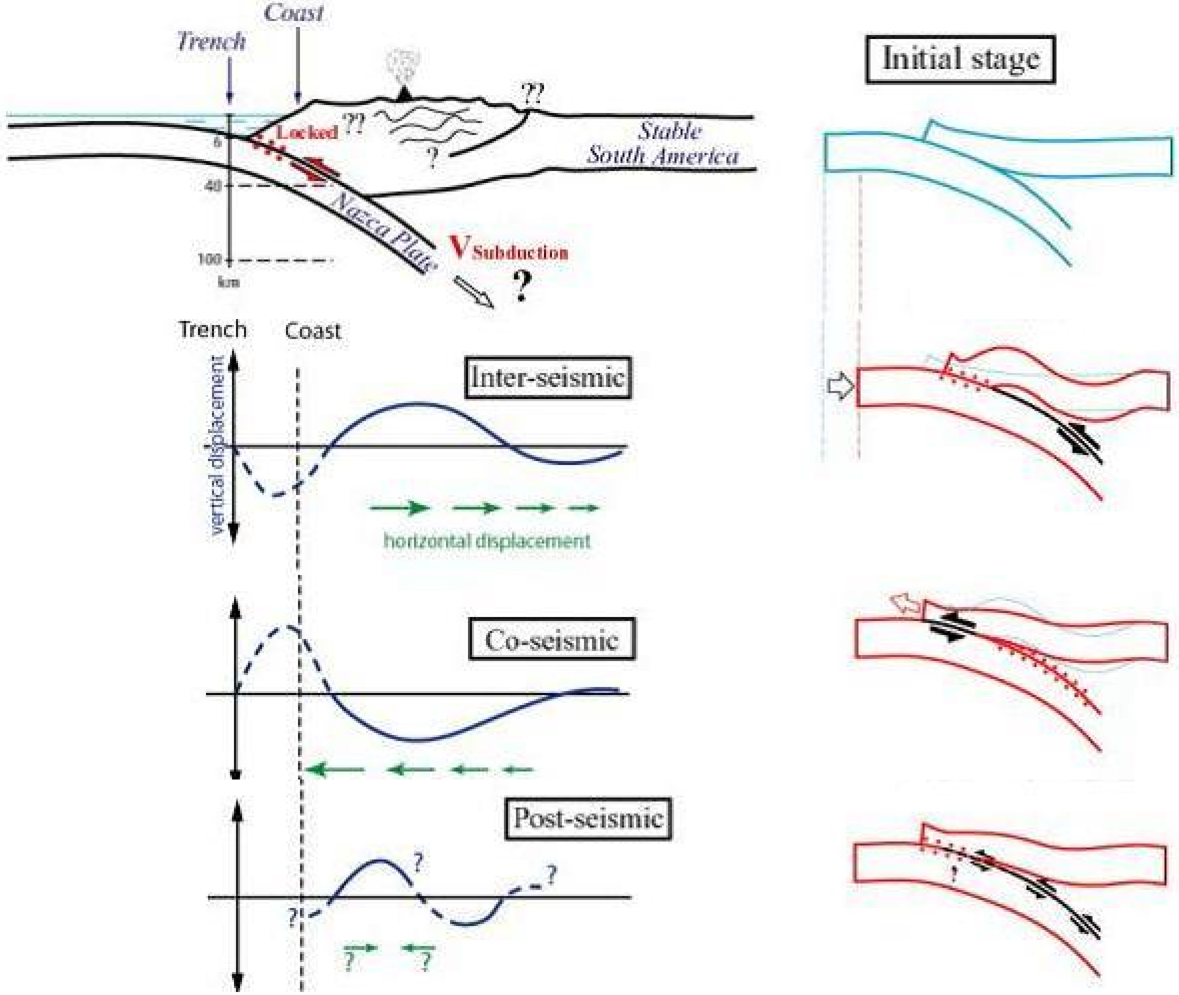

100^s years

seconds -> minutes

months- -> years

Size of an Earthquake

Earthquake « size » or released Energy E, is proportional to :

- Quantity of slip (U)
    - fault velocity (V) x time between earthquakes Δt
- Size of ruptured surface (S)
    - Length of rupure (L) x Locking depth of fault (d)

$$\boxed{\Rightarrow E = \mu \times S \times U = \mu \times L \times d \times V \times \Delta t}$$

Magnitude of an Earthquake :

$$\boxed{M = Log\,(E)}$$

Time & space dependant station motion

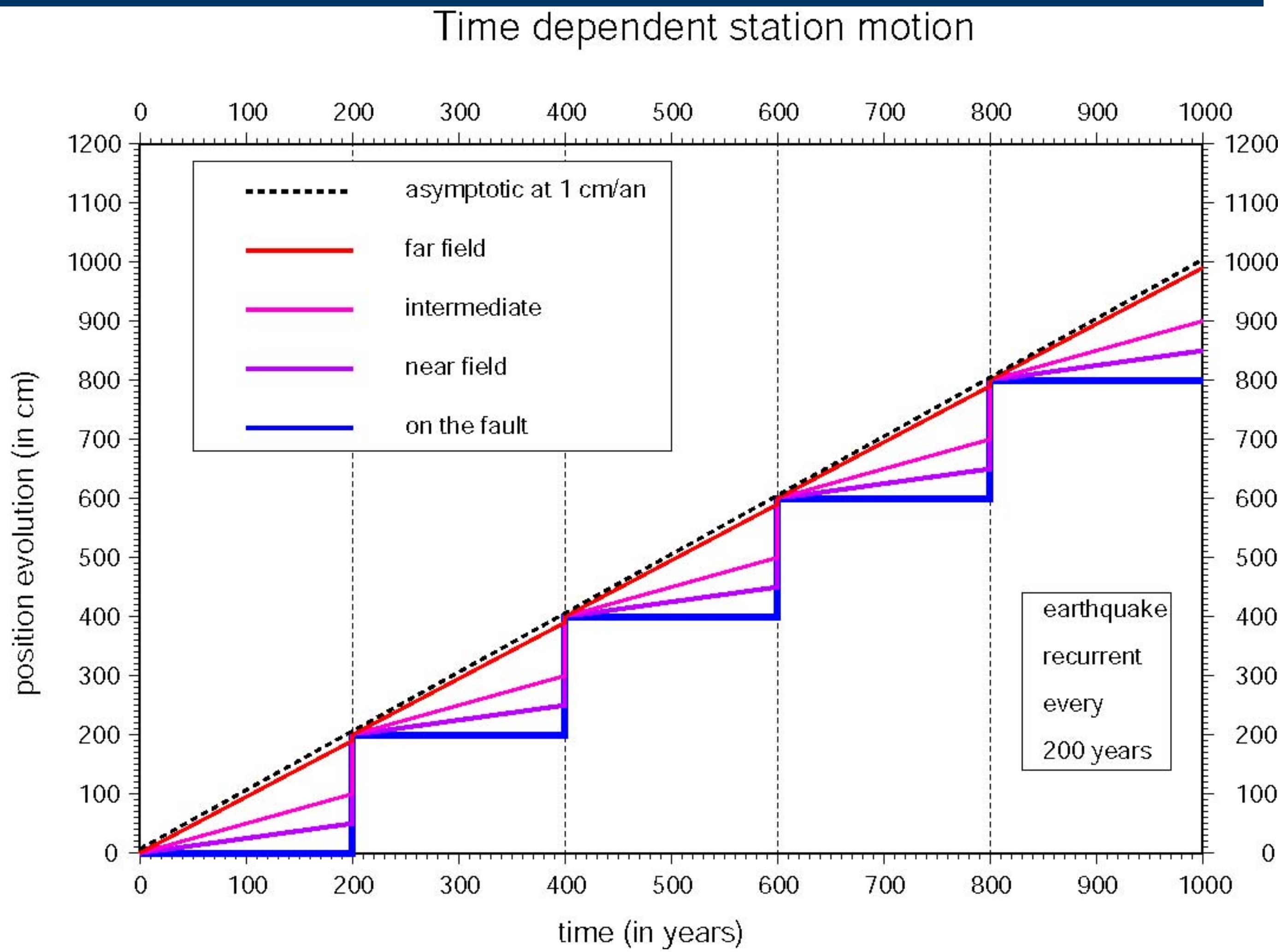

Earthquake cycle : Read and Wallace models

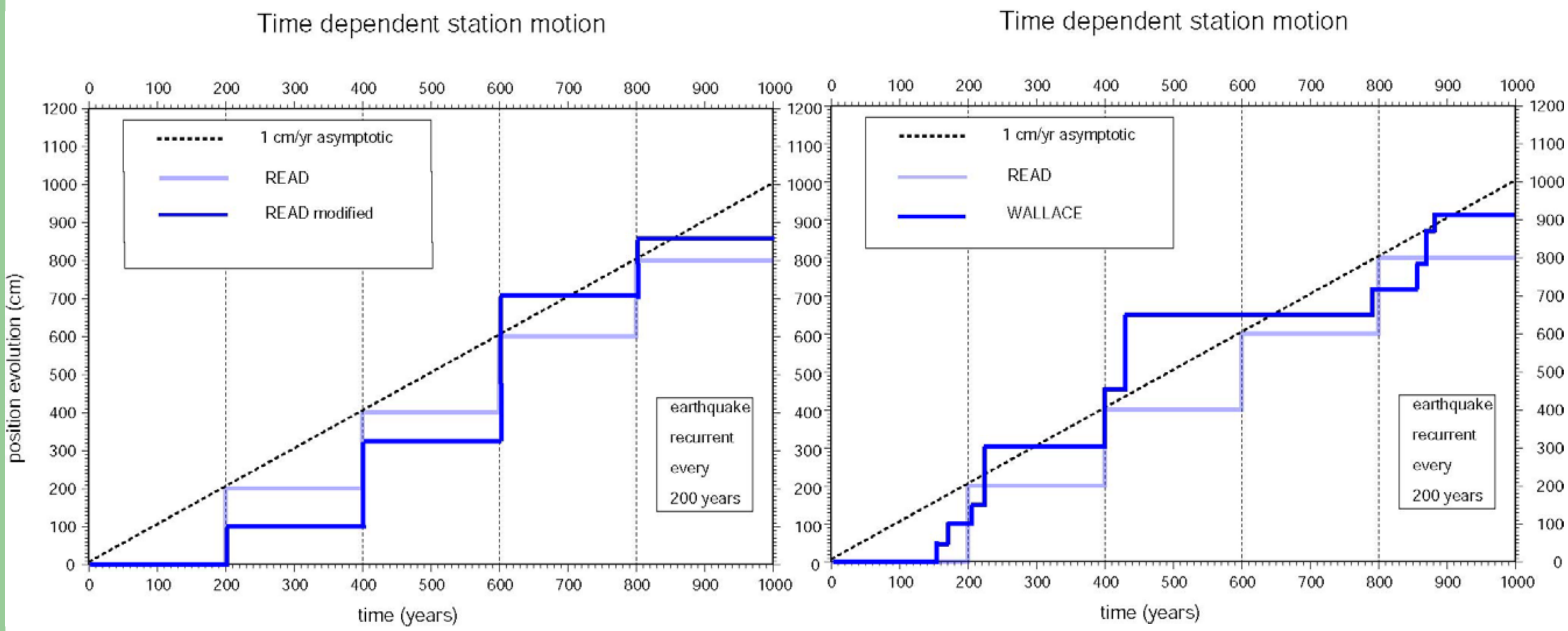

Difficulty of earthquake prediction

Even though a given fault can have a characteristic Earthquake repeating itself over a characteristic time, earthquake prediction is difficult because :

1. Those values can be **unknown**, especially if the characteristic time is very long
2. The earthquakes may occur at recurrence time interval, **plus or minus many decades (or centuries)**
3. Physical and/or rheological conditions may change with time and in particular **affected by earthquakes themselves**

Only lower bound of future Earthquake magnitude can be given, assuming :

a. time of latest event

b. Current velocity on fault

c. Locking depth of fault

Guttenberg-Richter Law

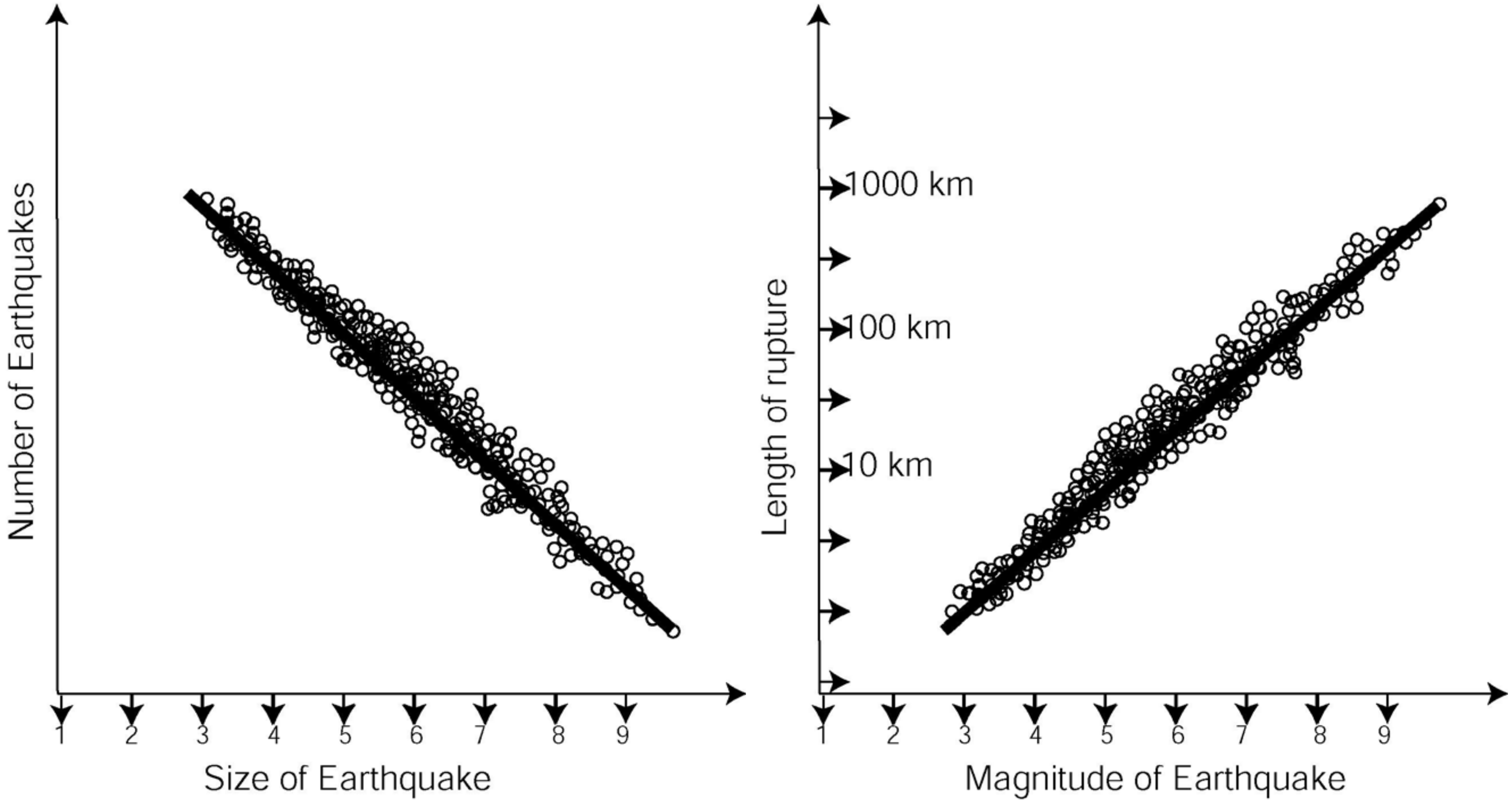

A fault of given length will give an earthquake of given magnitude

Zooming around earthquakes

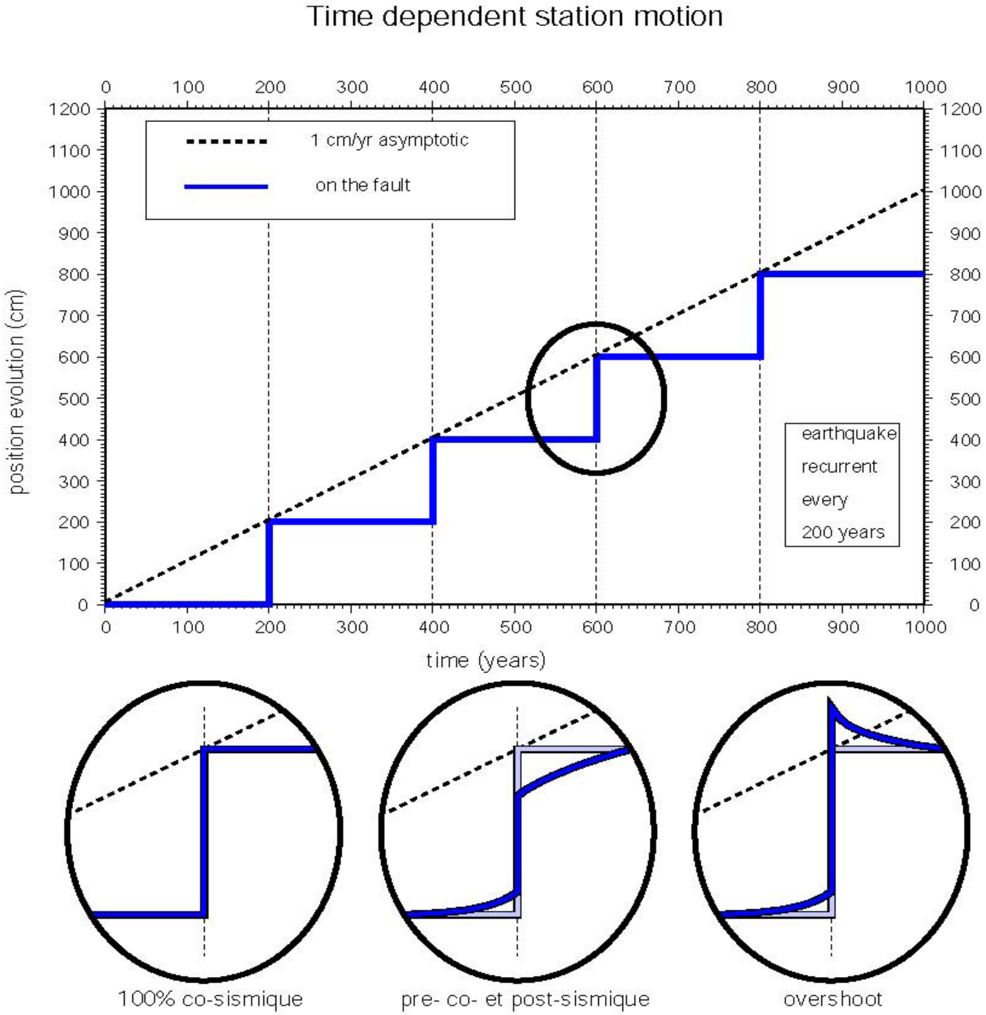

Post-seismic : K. HEKI, Nature 1997

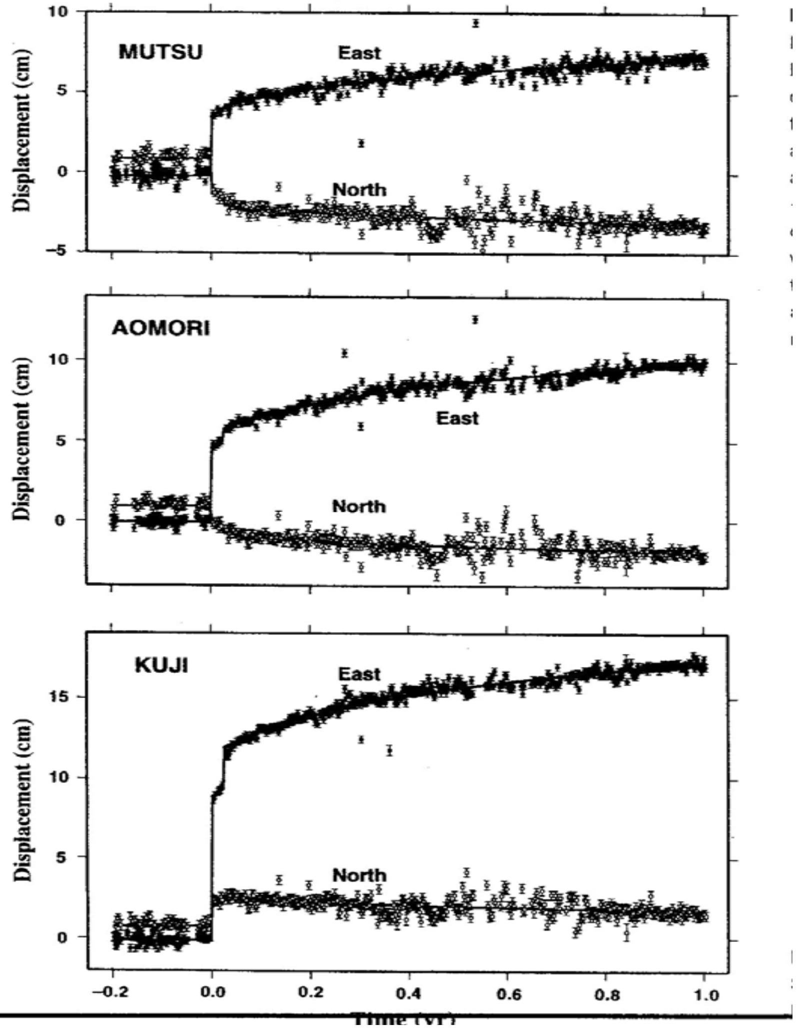

Silent fault slip following an interplate thrust earthquake at the Japan trench

Horizontal coordinate time series before and after the **1994 Sanriku-haruka-Oki earthquake** observed at three GPS stations : Mutsu, Aomoriand and Kuji. Dots denote north and east components. Black lines are the model curves (stationary for t < 0, logarithmic decay for t > 0, discontinuity for t= 0).

Sanriku-Haruka-Oki sequence

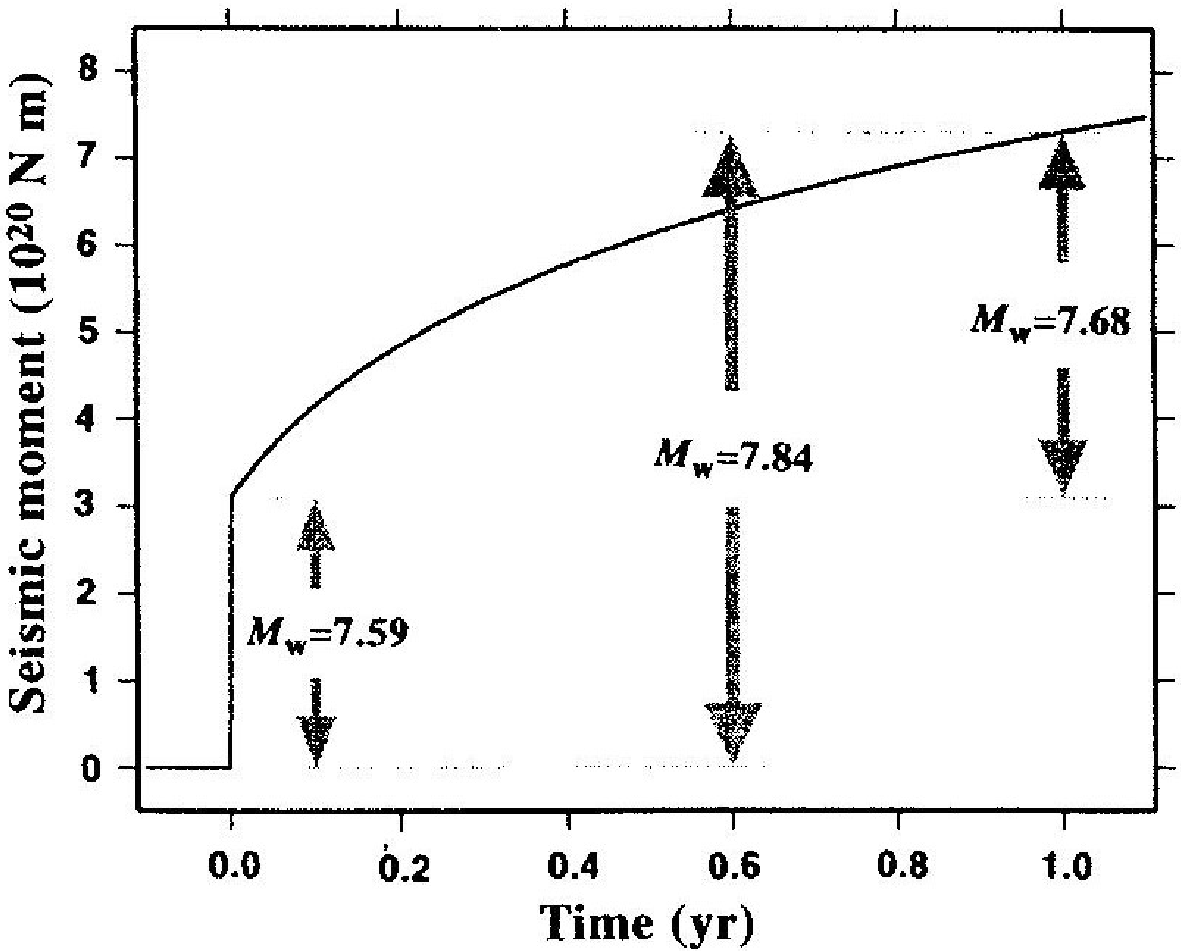

20+ years of Post seismic in Afar Rift

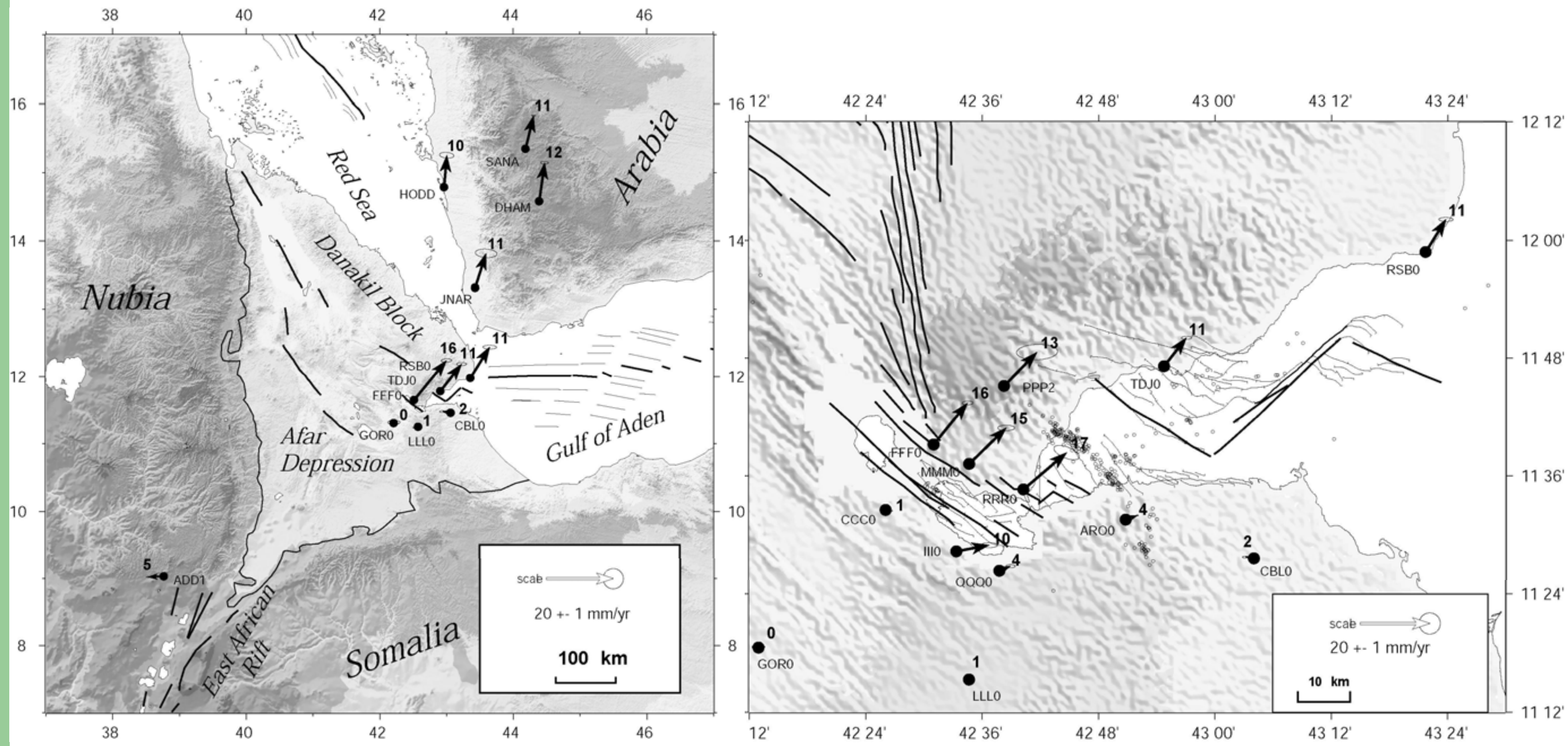

20+ years of Post seismic in Afar Rift

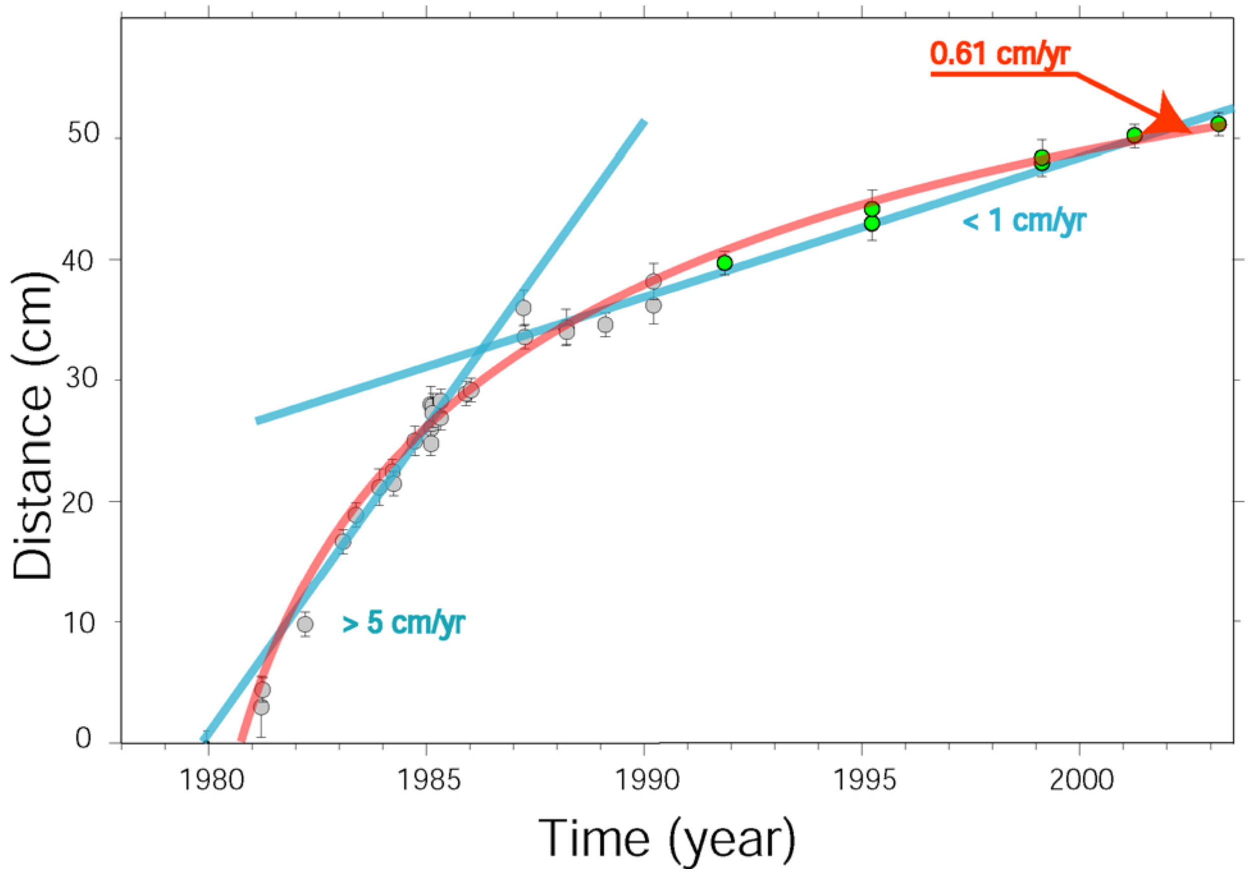

Co-seismic (in 1979) = 1.5 m

Viscous relaxation = 50 cm

Present day velocity : +6.1 mm/yr

Far field velocity : +11 mm/yr

Accumulation : ~5 mm/yr

=> Next crisis in 300 years ?

GPS time series

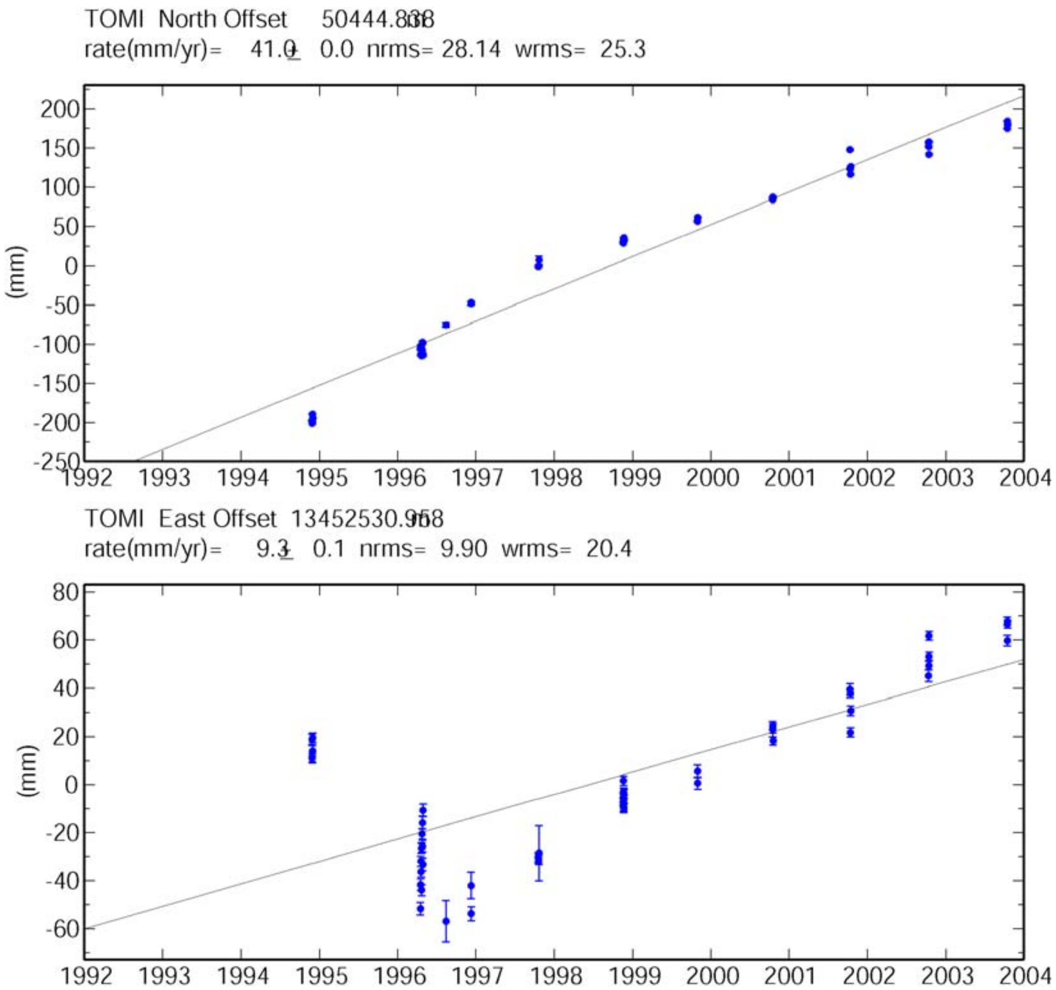

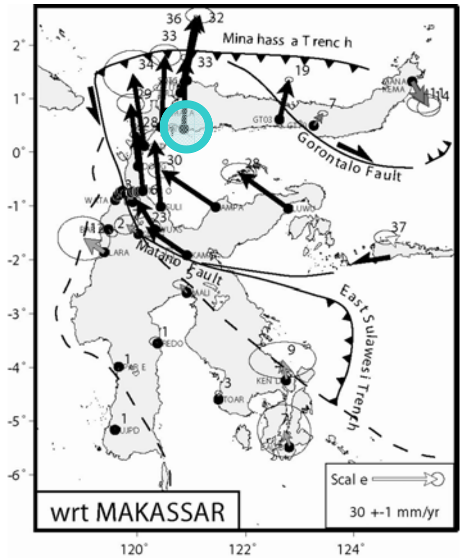

Post seismic relaxation model

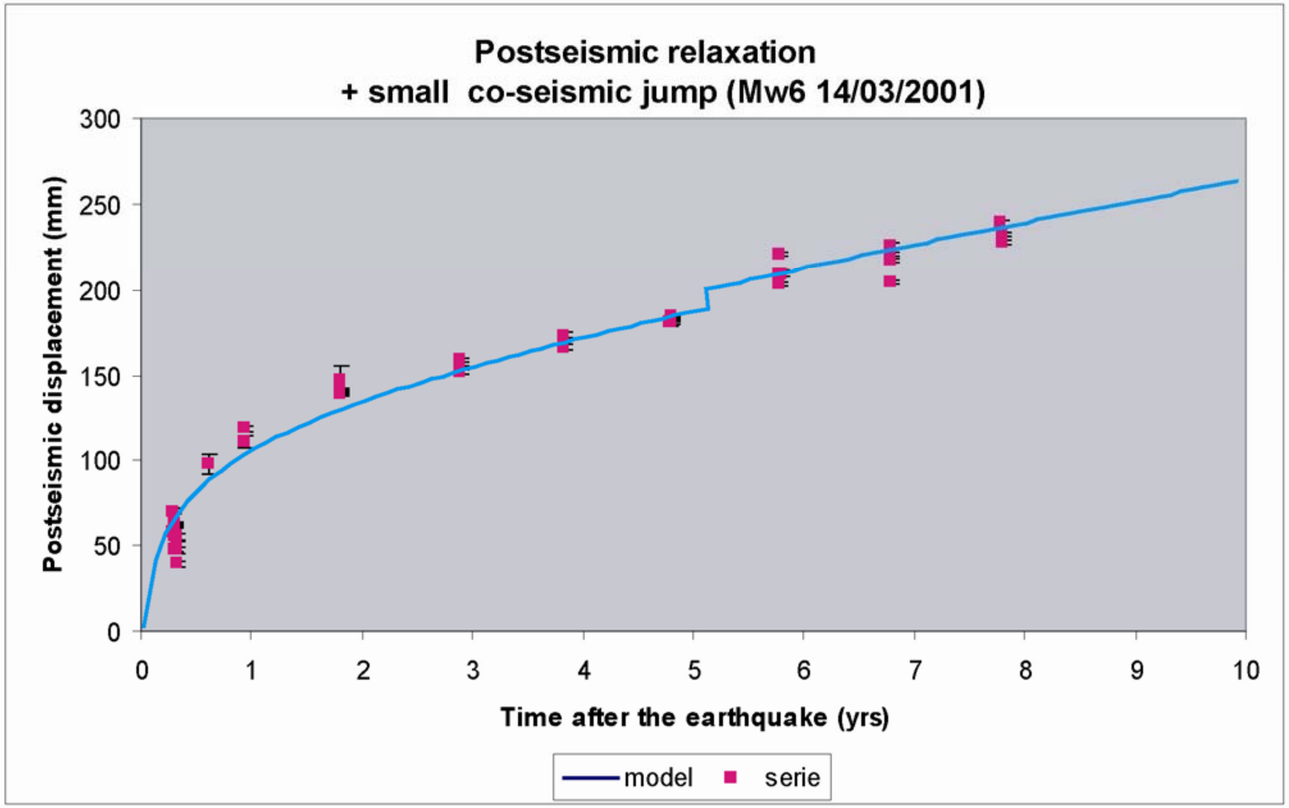

ToliToli Continuous station

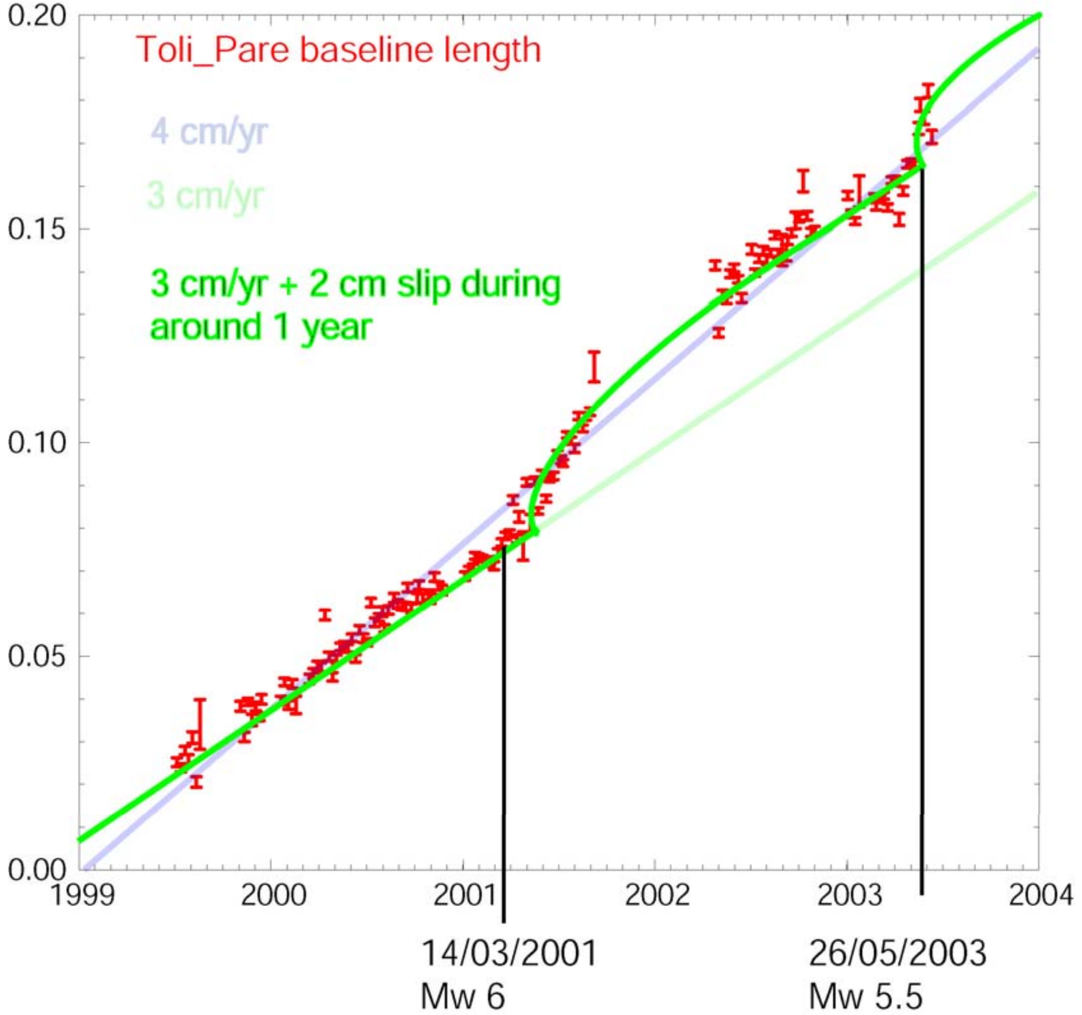

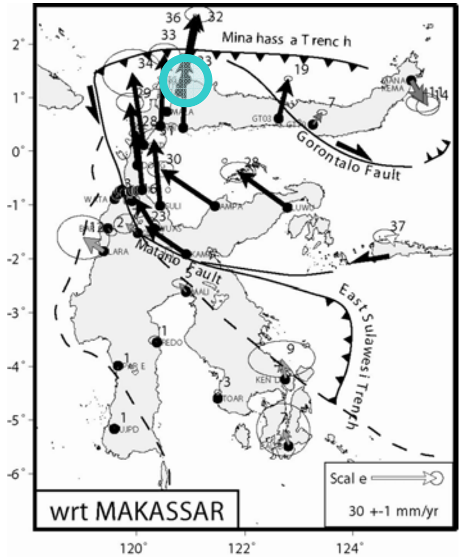

Silent slip on Cascadian subduction zone

Dragert et al., Science, 292, May 2001

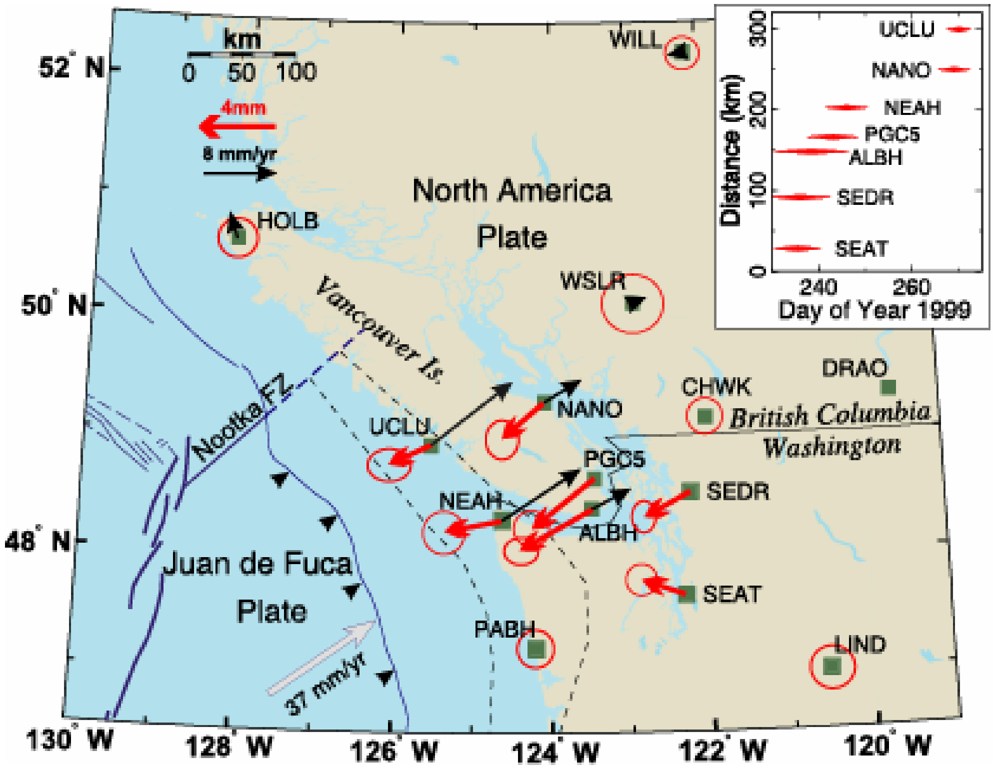

Fig. 1. Location of continuous GPS sites that are included in the routine analysis of GPS data carried out at the Geological Survey of Canada (GSC). Sites in Canada are operated and maintained by the GSC; U.S. sites, which form part of the PANGA (Paciﬁc Northwest Geodetic Array) network, are operated by a consortium of university and government agencies. Bold (red) arrows show displacements (with respect to DRAO) due to the slip event. Error ellipses are double the 95% conﬁdence limits derived from the formal regression errors of Table 1. Thin (black) arrows show 3- to 6-year average GPS motions with respect to DRAO (7). The two dashed lines show the nominal downdip limits of the locked and transition zones from the model of Fluck et al. (20). Inset shows the approximate time interval of the transient signal at each site along a northwest-striking line.

Jump in time series

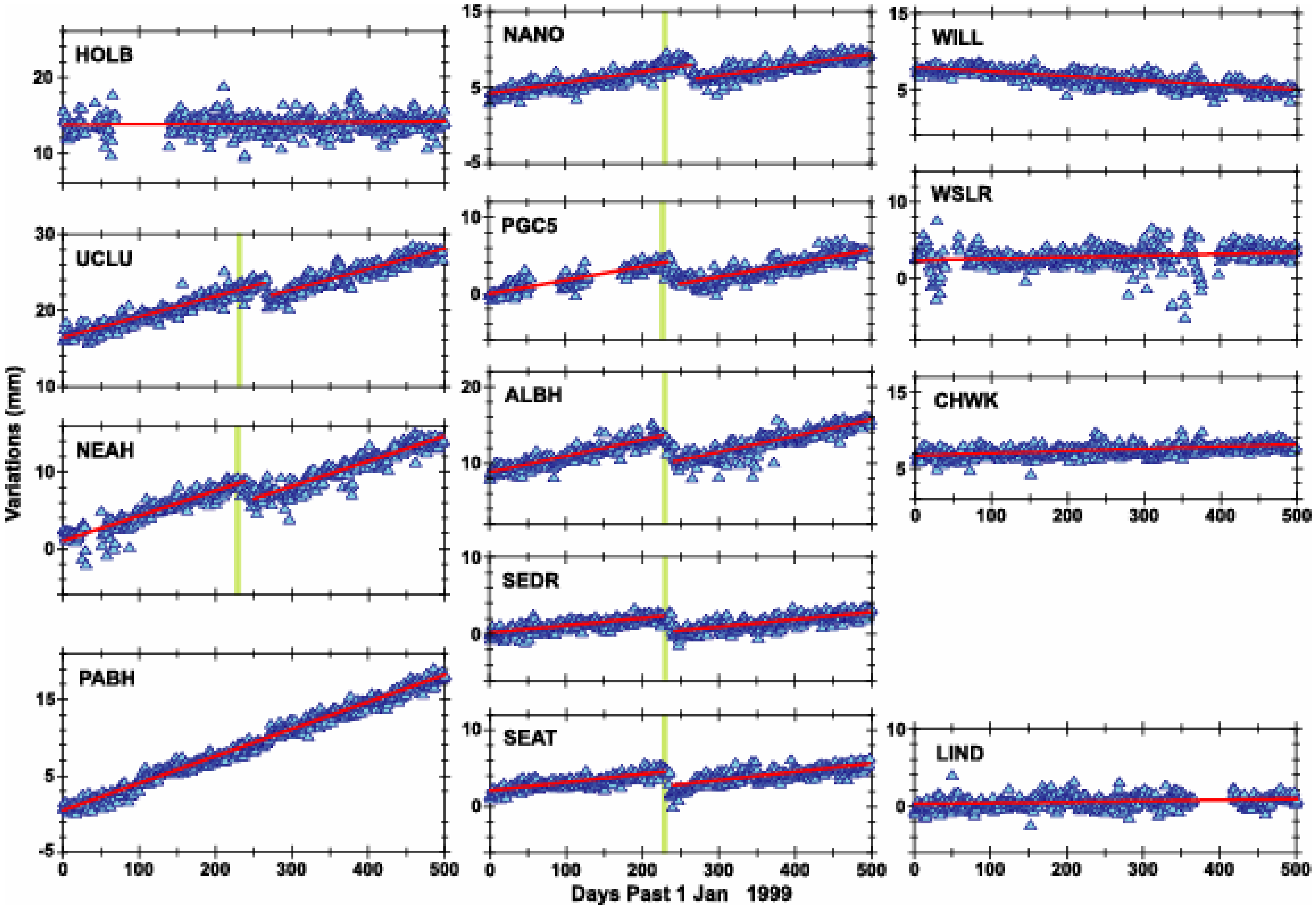

Fig. 3. Filtered
series of daily
tions in relative
tude with respect
DRAO. Annual
have also been
moved. Red lines
the best-Þtting
trends, which
sumed constant
fore and after
transient. The
green bars indicate
the earliest date
detection (day
the transient.

Silent slip on subduction interface

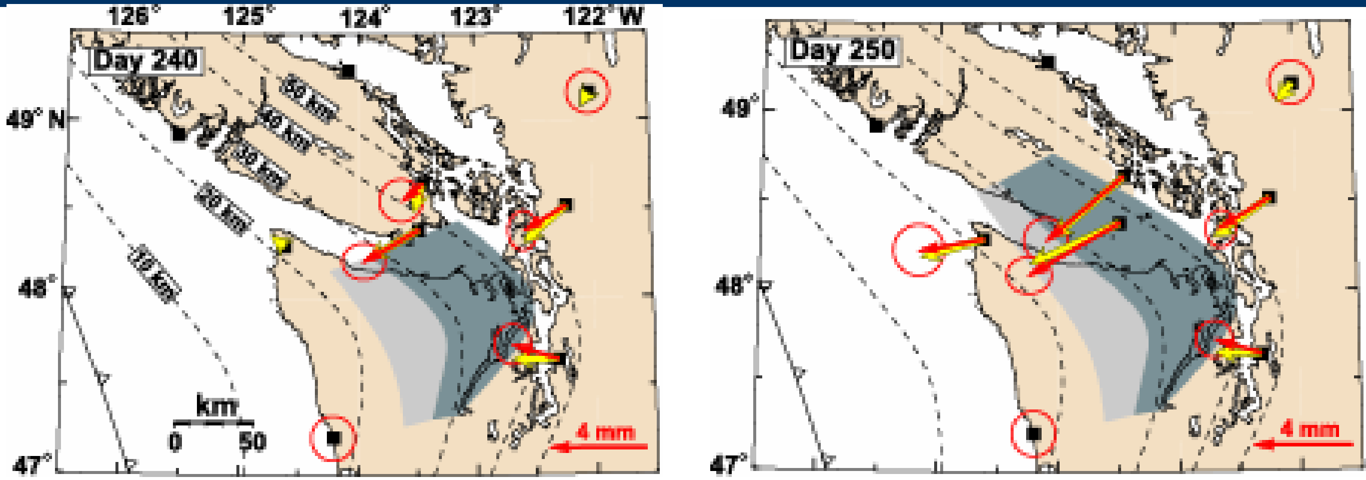

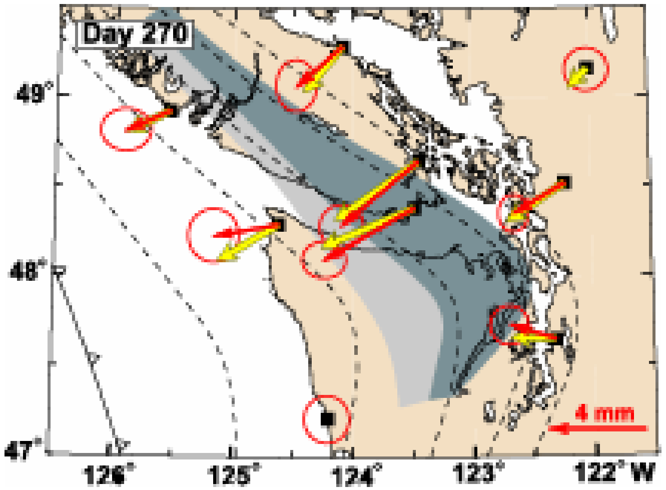

Fig. 4. Three-dimensional model of slip on the subduction interface. Dashed lines are depth contours of the interface. Slip direction is set constant at 235¡, the direction of motion of the North America plate with respect to the Juan de Fuca plate. Dark shading indicates the plate interface area with full (2.1 cm) slip; lighter shading indicates area where slip tapers linearly from 2.1 cm to 0 cm updip. Panels, marked by the day of year 1999, show the total area of slip on the interface in three time slices and the commensurate evolution of the surface displacement vectors [broad (yellow) 5 model; thin (red) with error ellipses 5 observed]. Day 240 is within the time interval of the GPS transient at PGC5 and ALBH, and their observed displacement vectors have been scaled, assuming a linear increase of the displacement with time.

McGuire and Segall, G.J.Int. ,2003.

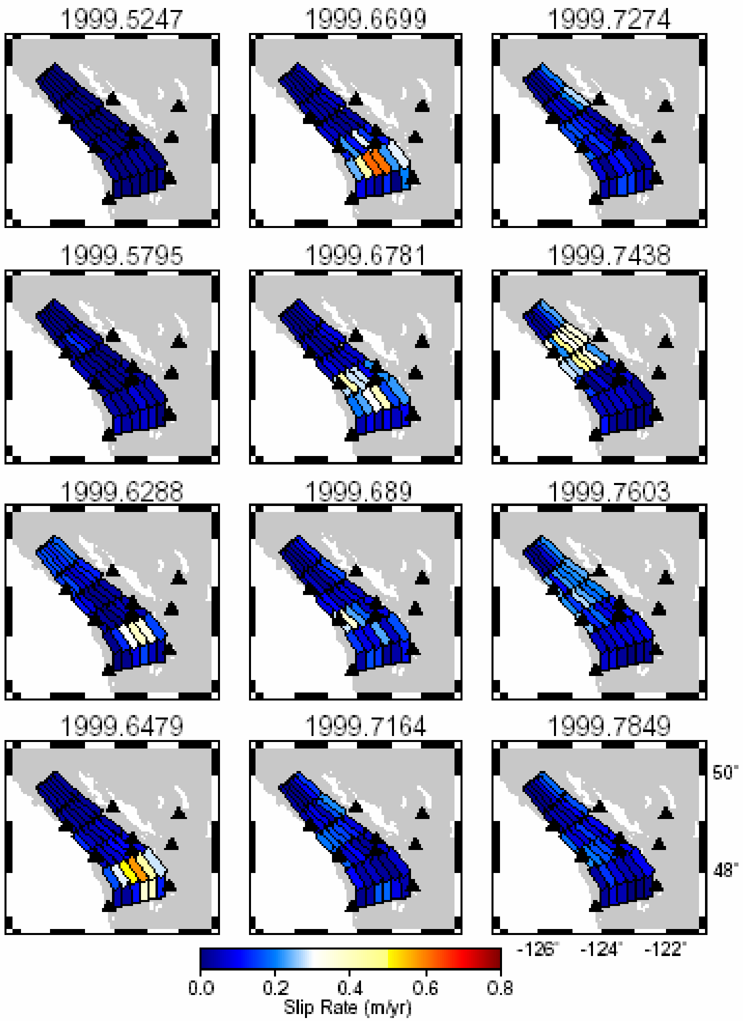

Maps of the estimated slip-rate as a function of time and station distribution (black triangles).

Ruegg et al., 2001, *seismological research letters*

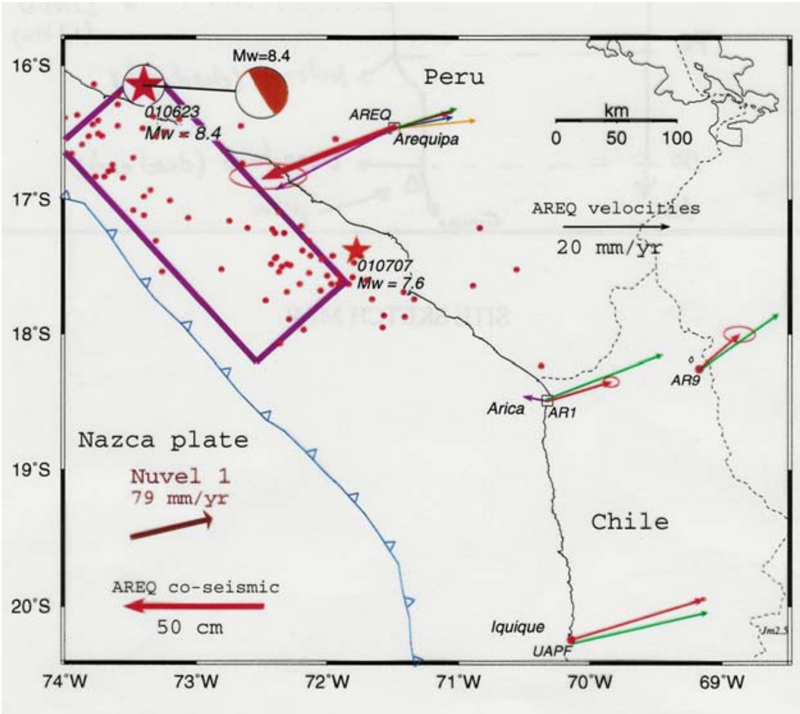

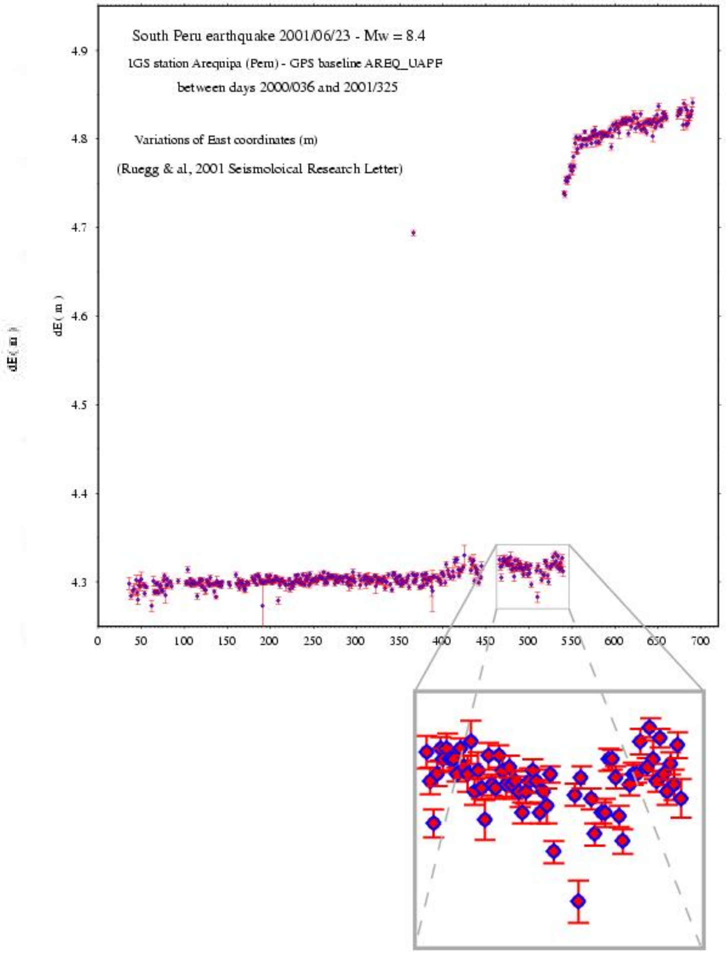

Towards detection of
preseismic motion

Clustering of Earthquakes

Landers1.swf

Southern California seismicity, 1981-2004, in 4-months increments

Observed seismicity in 4-month time increments in a 300 x 310 km area of southern California centered on the 1992 Landers rupture. Red lines in the time scale at left mark the times of mainshocks; their epicenters (stars) and fault ruptures (bold red lines) briefly appear. While the background seismicity pattern is remarkably stable, it is punctuated by mainshocks and their rapidly decaying aftershocks. Because the majority of aftershocks occur in the first frame after each main shock, it is difficult to judge how aftershock zones grow, migrate, or change.

Earthquake Stress increase

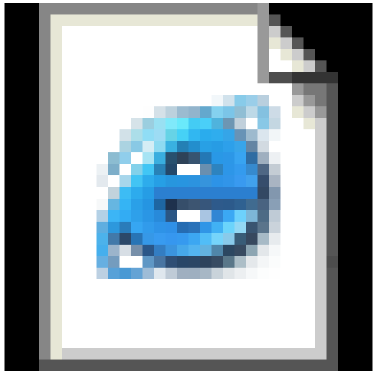

Grid.swf

An earthquake reduces the average value of the shear stress on the fault that slipped, but shear stress rises at sites in addition to the fault tips (Chinnery, 1963).
lobes of off-fault aftershocks were seen to correspond to small calculated increases in shear or Coulomb stress.

Coulomb stress increase

$$\Delta\sigma_f = \Delta\tau + \mu\,(\Delta\sigma_n + \Delta P)$$

Coulomb failure stress change

Shear stress change on the fault

normal stress change on the fault

Pore pressure change on the fault

"Friction" coefficent

Failure is promoted if ΔCF increases

Pore pressure (> with pressure) counteracts normal stress (> if unclamped)

How the Coulomb Stress Change is Calculated

Stress Rise Drop

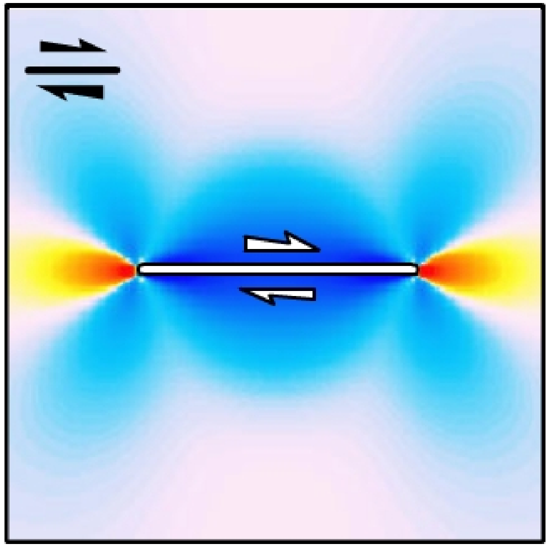

Shear stress
change

$\Delta\tau_s$

- Example calculation for faults parallel to master fault

From King et al (BSSA, 1994)

How the Coulomb Stress Change is Calculated

Stress Rise *Drop*

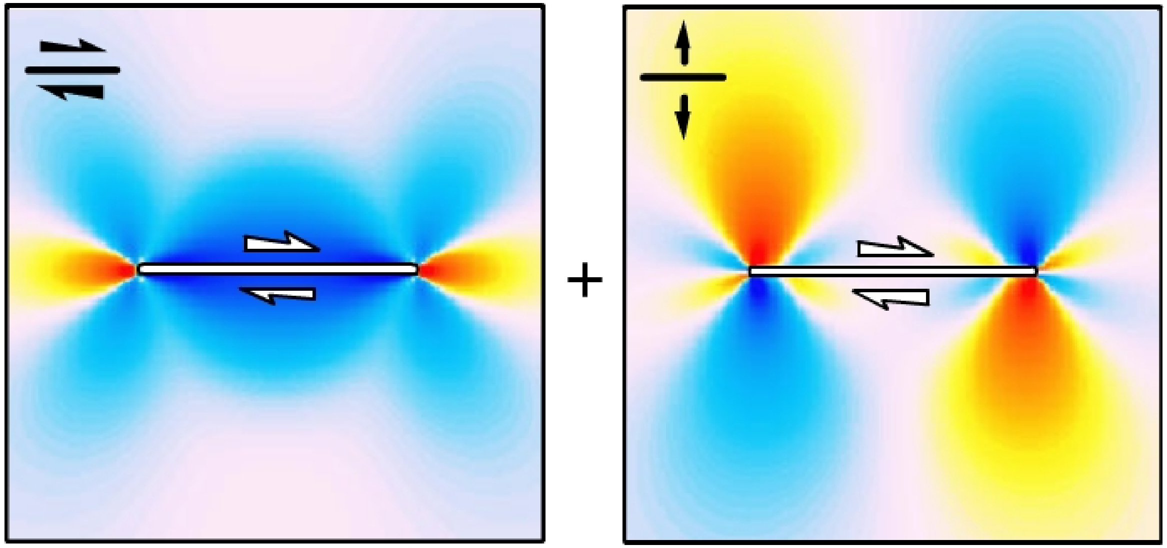

Shear stress change + Friction coefficient **x** normal stress change

$$\Delta\tau_s \quad + \quad \mu' \, (\Delta\sigma_n)$$

- Example calculation for faults parallel to master fault

From King et al (BSSA, 1994)

How the Coulomb Stress Change is Calculated

Stress *Rise* *Drop*

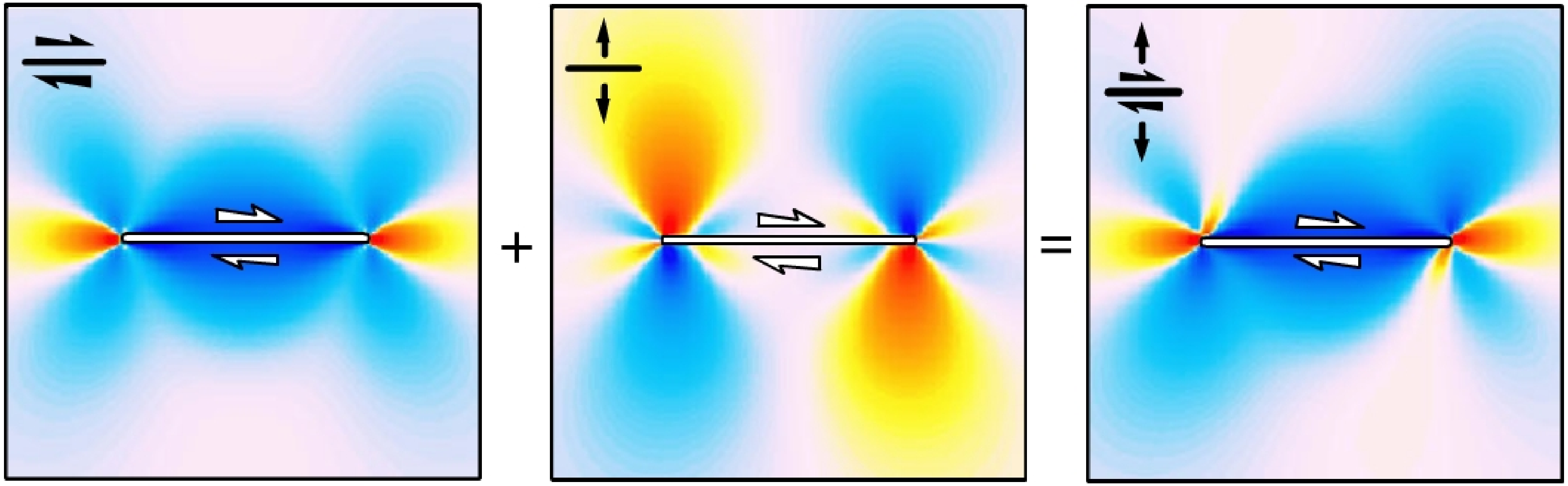

Shear stress change	+	Friction coefficient **x** normal stress change	=	Coulomb failure stress change
$\Delta\tau_s$	+	$\mu' (\Delta\sigma_n)$	=	$\Delta\sigma_f$

- Example calculation for faults parallel to master fault

From King et al (BSSA, 1994)

Coulomb stress imparted by mainshocks

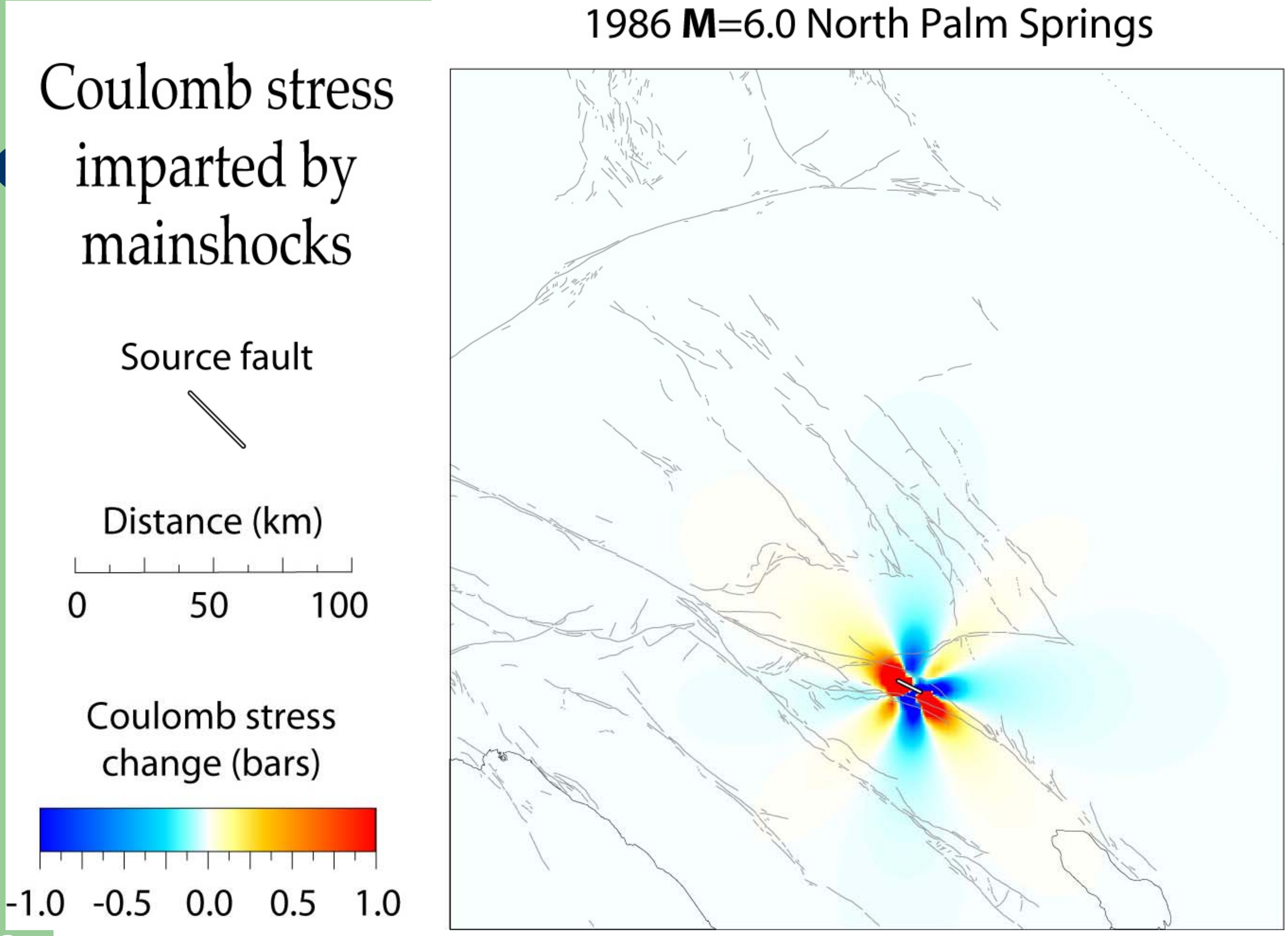

from Todal et al (JGR, 2005)

Coulomb stress imparted by mainshocks

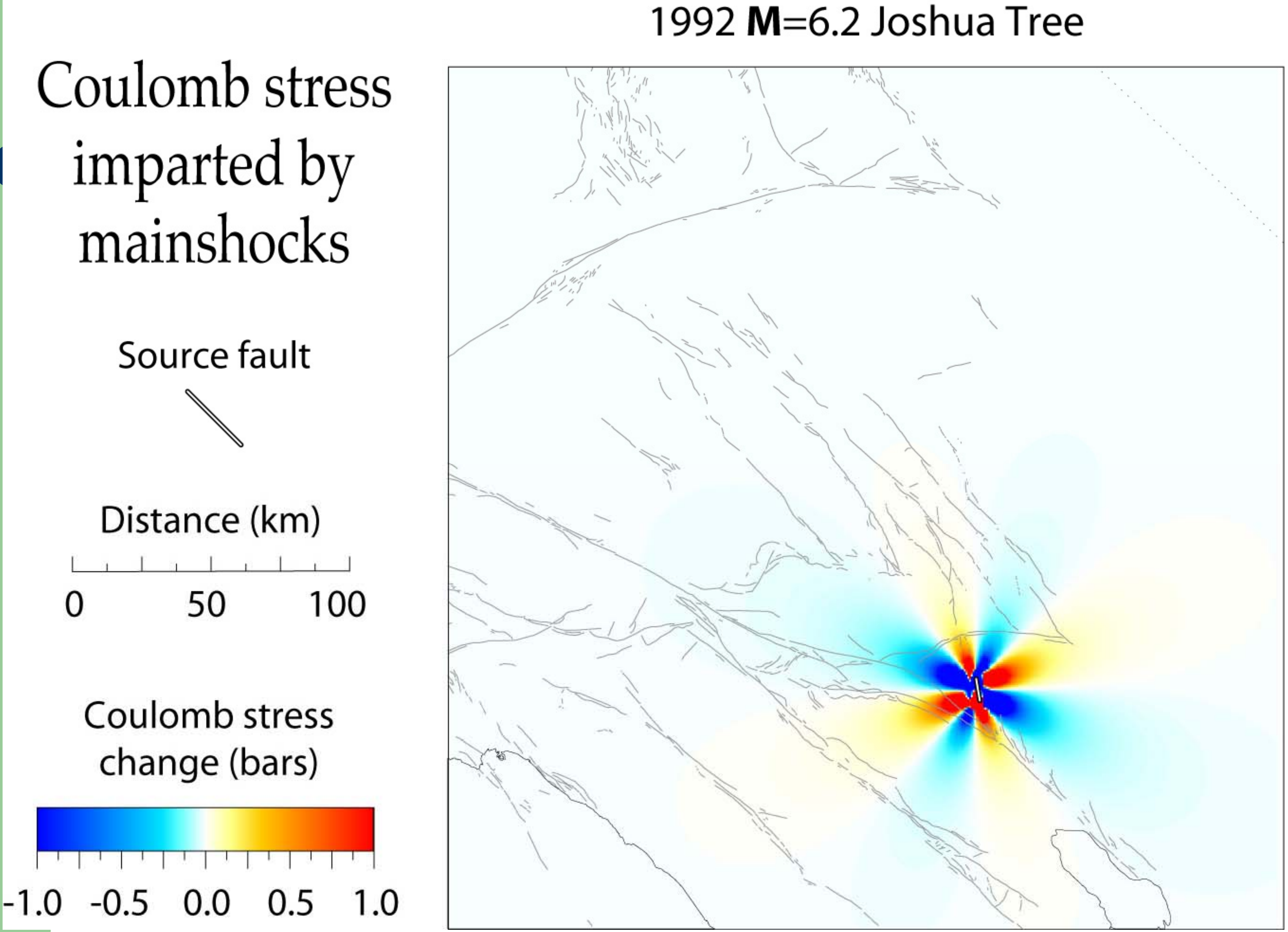

from Todal et al (JGR, 2005)

Coulomb stress imparted by mainshocks

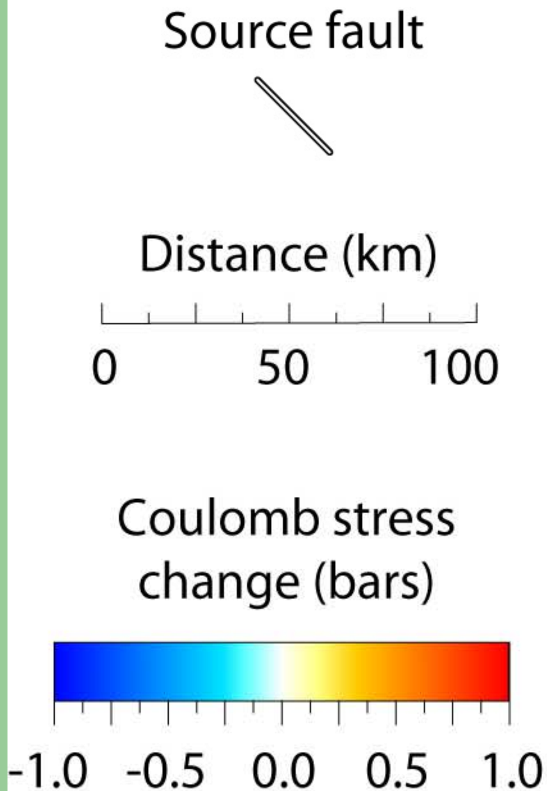

1992 **M**=7.4 Landers

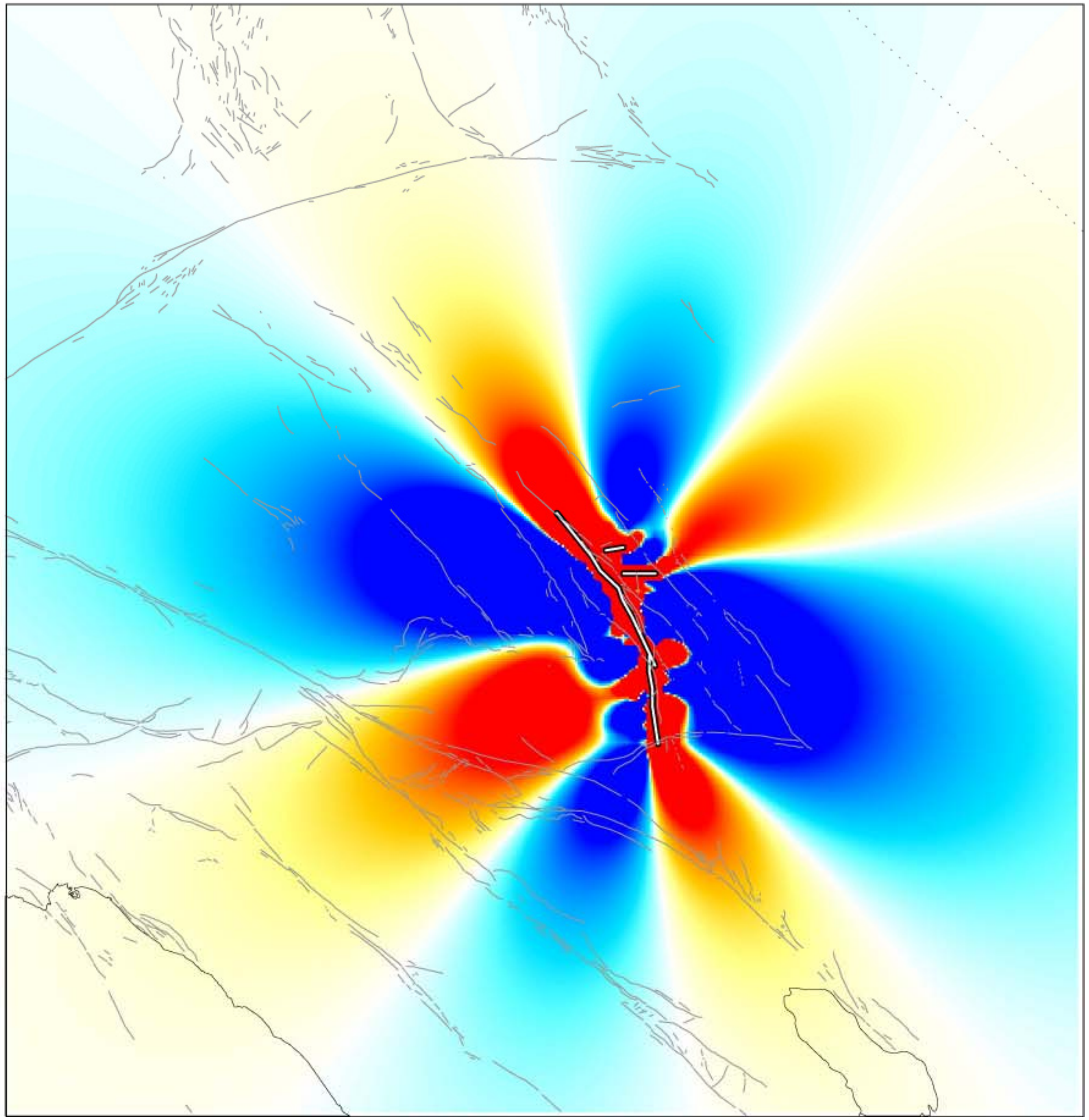

from Todal et al (JGR, 2005)

Coulomb stress imparted by mainshocks

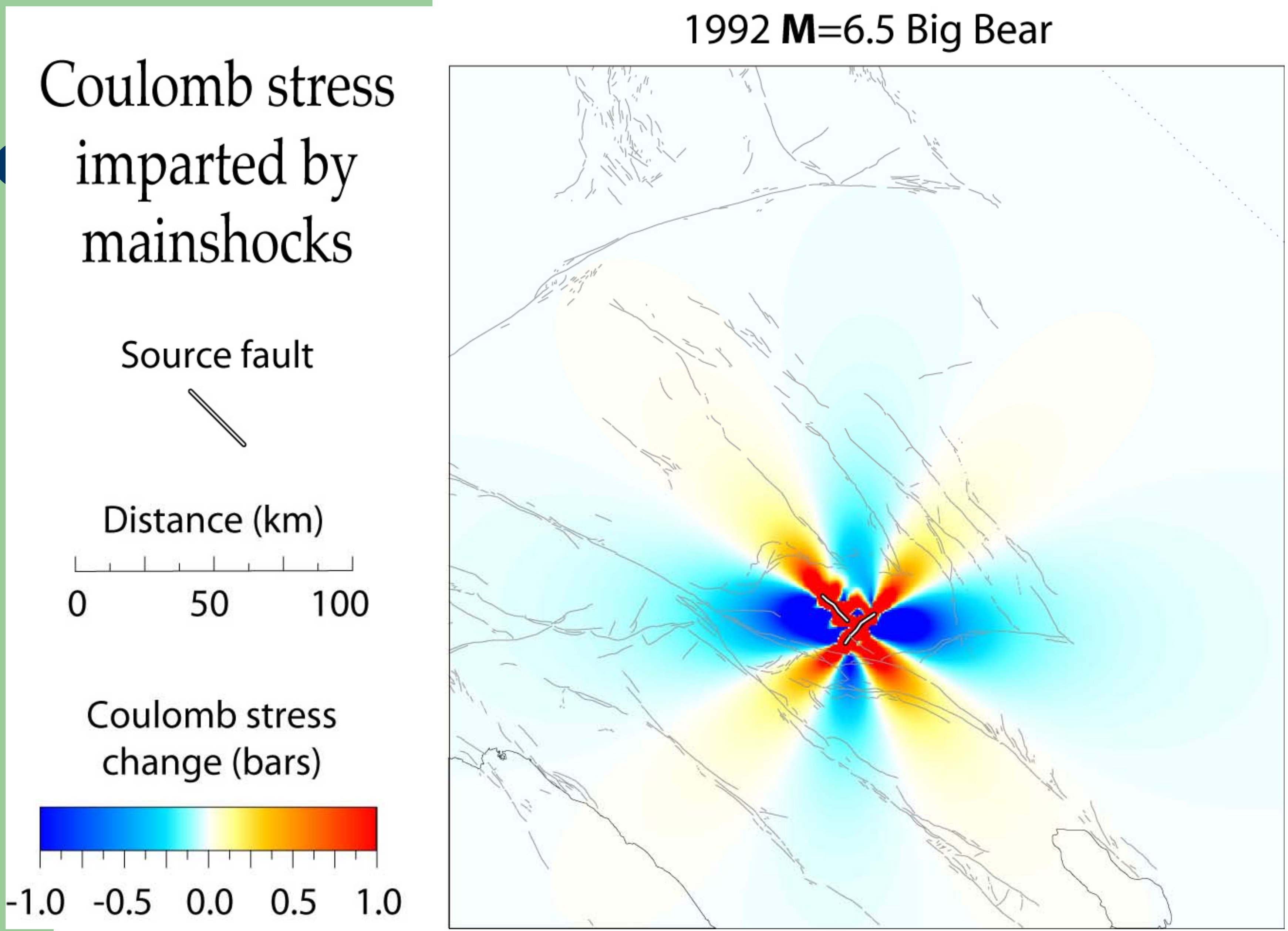

from Todal et al (JGR, 2005)

Coulomb stress imparted by mainshocks

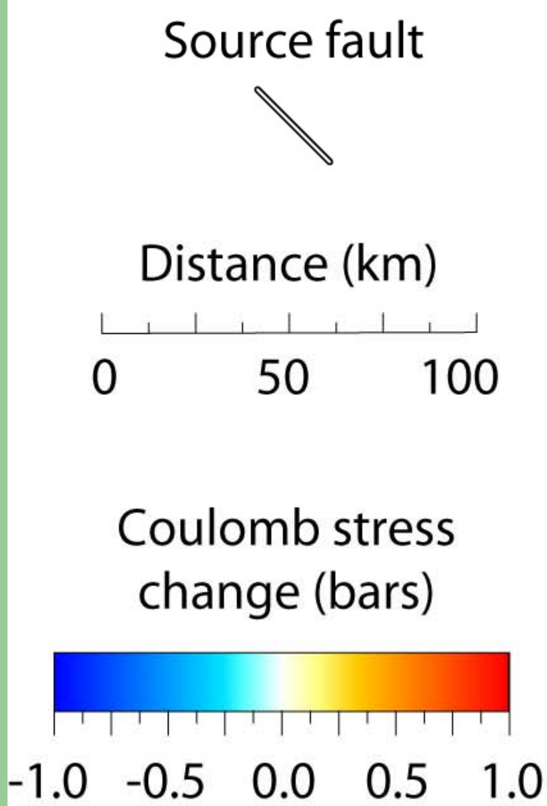

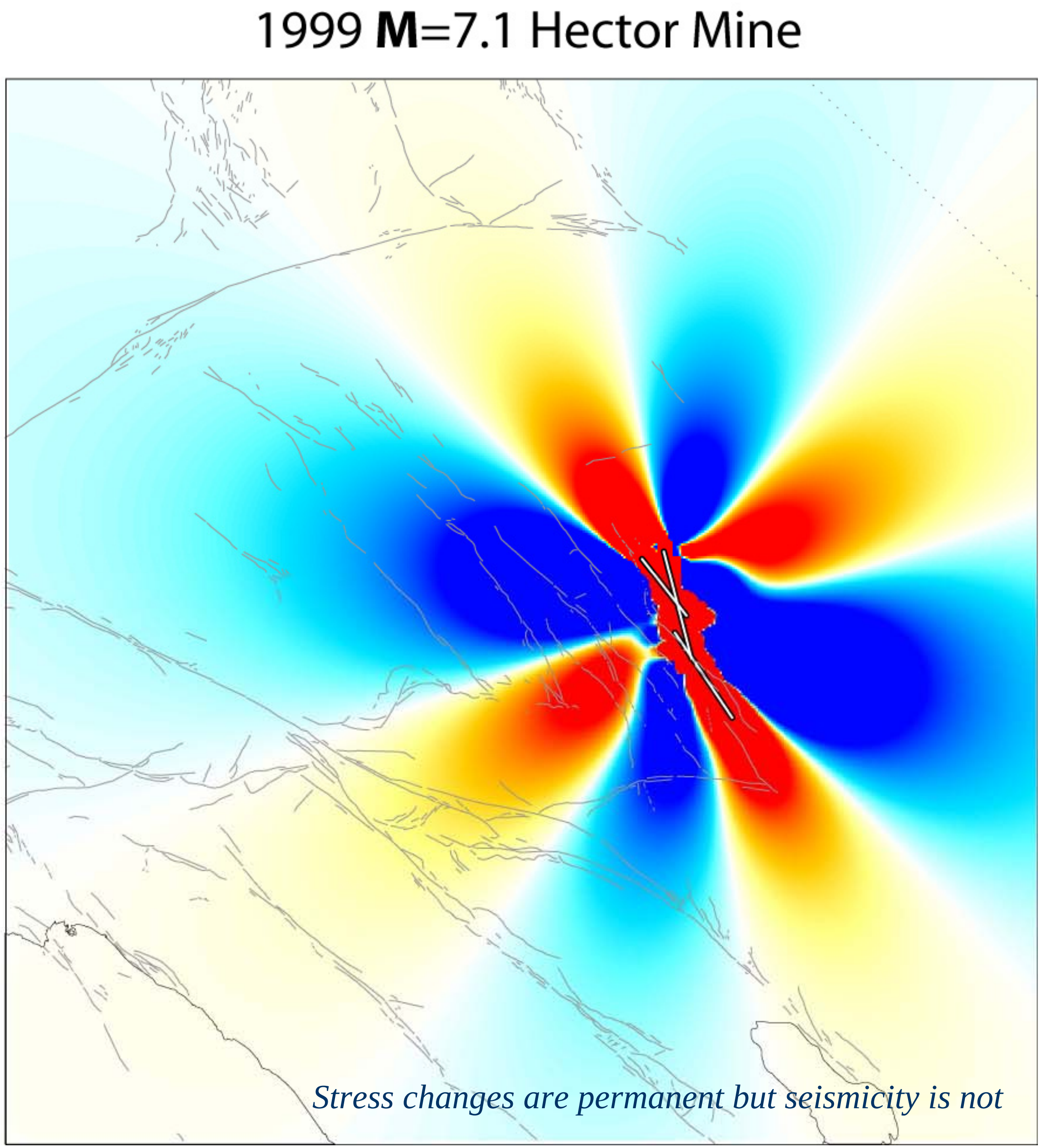

from Todal et al (JGR, 2005)

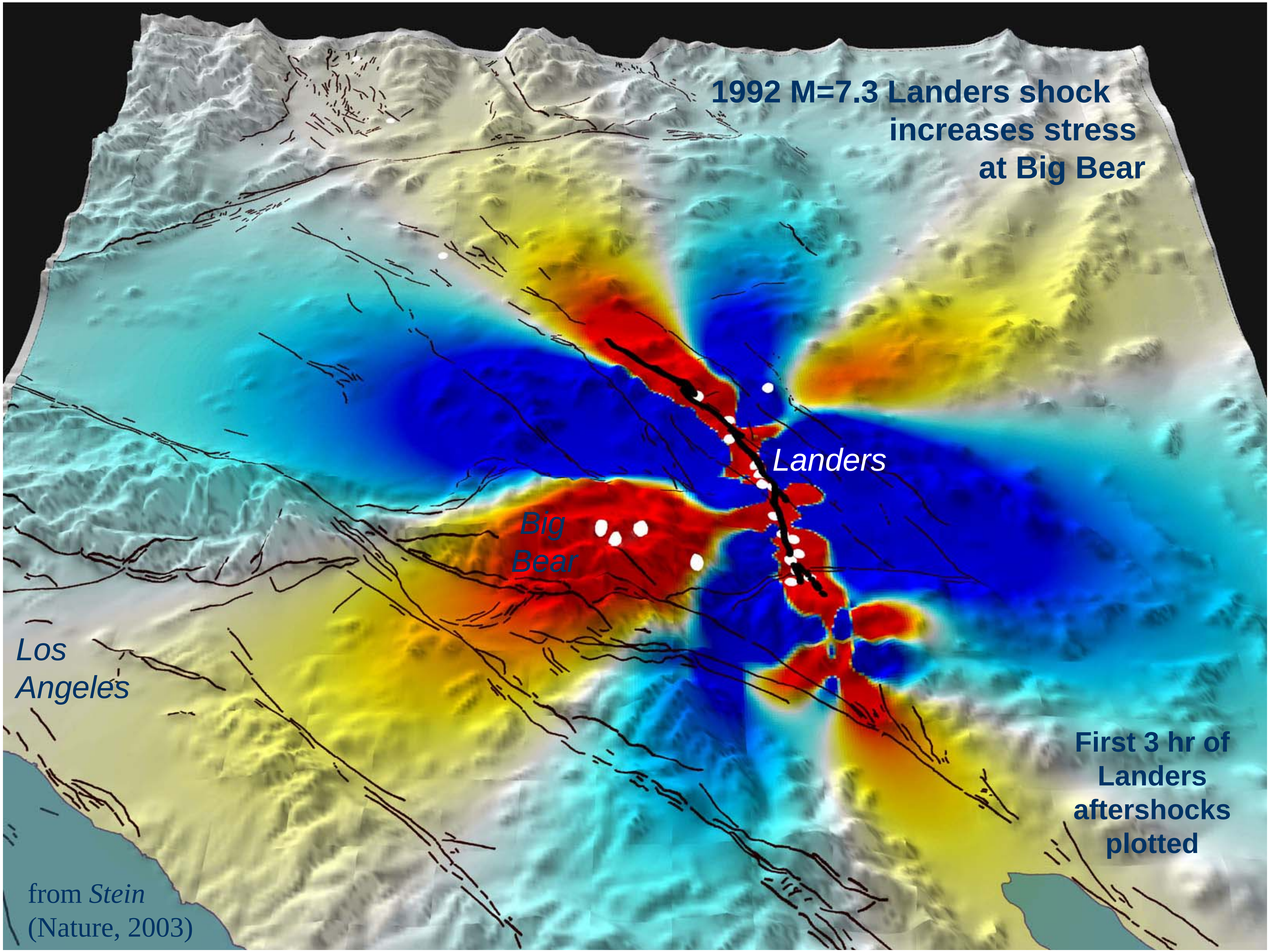
1992 M=7.3 Landers shock
increases stress
at Big Bear
Landers
Big
Bear
Los
Angeles
First 3 hr of
Landers
aftershocks
plotted
from Stein
(Nature, 2003)

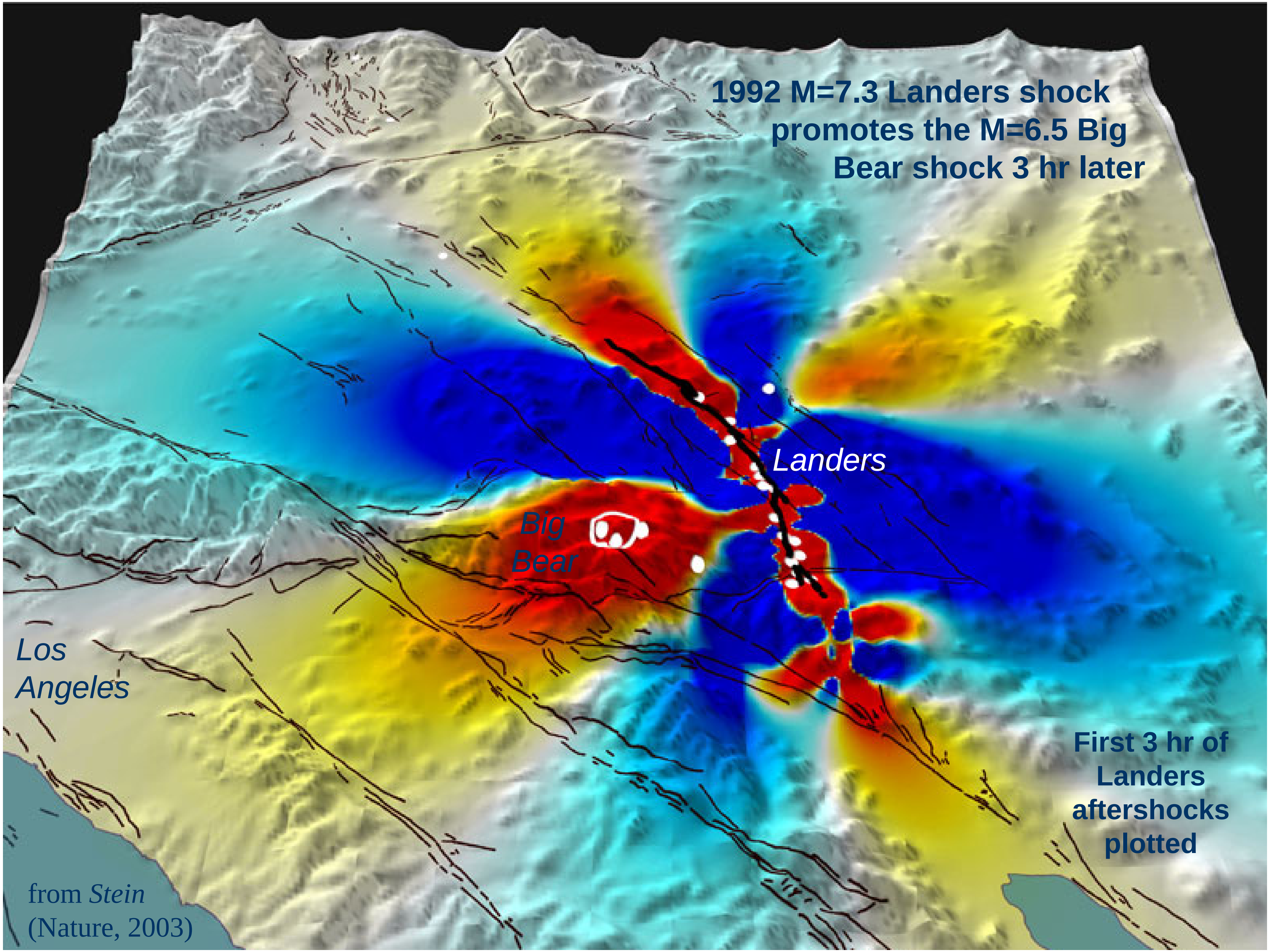
1992 M=7.3 Landers shock promotes the M=6.5 Big Bear shock 3 hr later
Landers
Big Bear
Los Angeles
First 3 hr of Landers aftershocks plotted
from *Stein* (Nature, 2003)

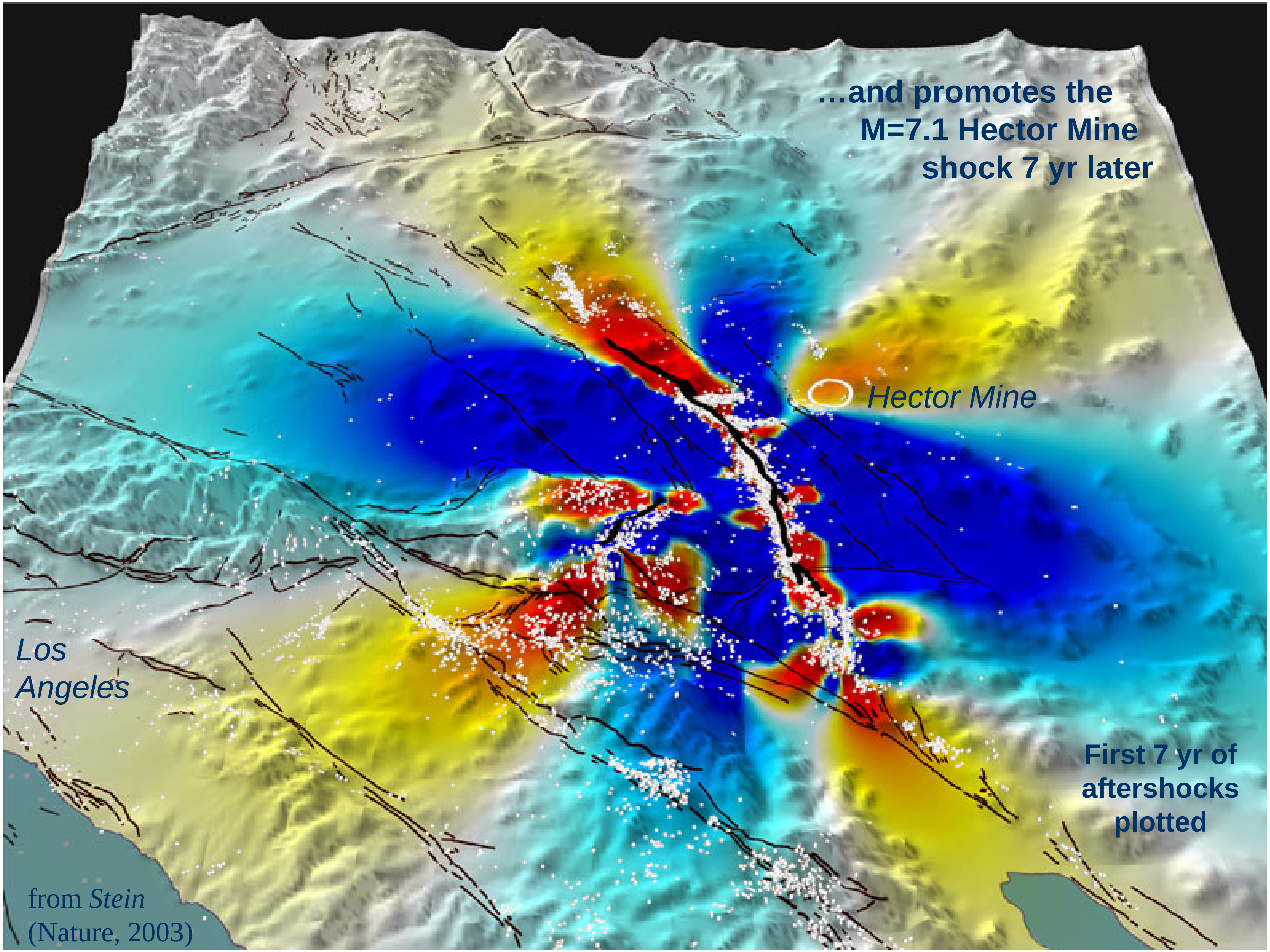

...and promotes the
M=7.1 Hector Mine
shock 7 yr later
Hector Mine
Los
Angeles
First 7 yr of
aftershocks
plotted
from *Stein*
(Nature, 2003)

New Idria aftershocks

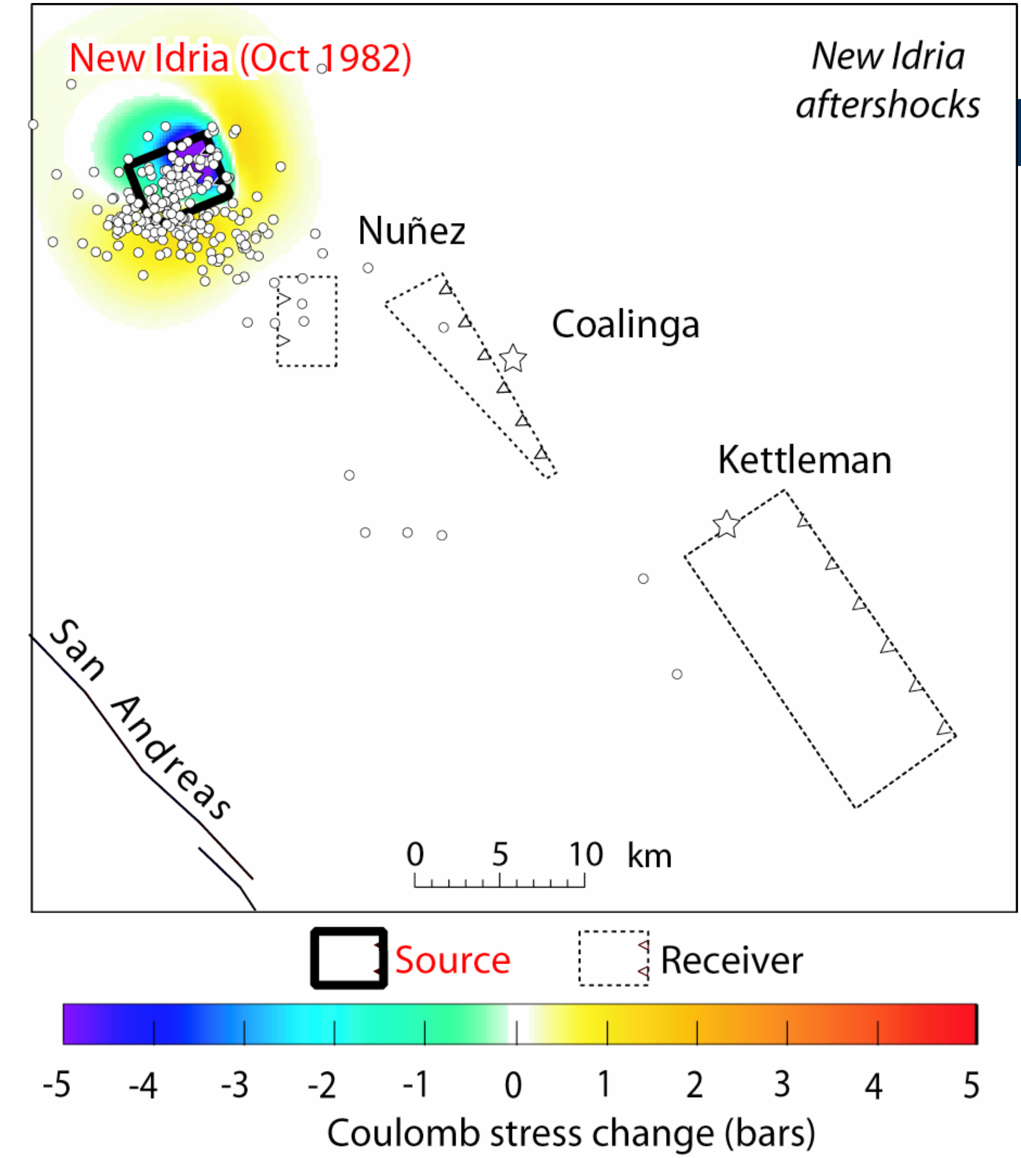

from *Lin & Stein* (JGR, 2004)

Coalinga aftershocks

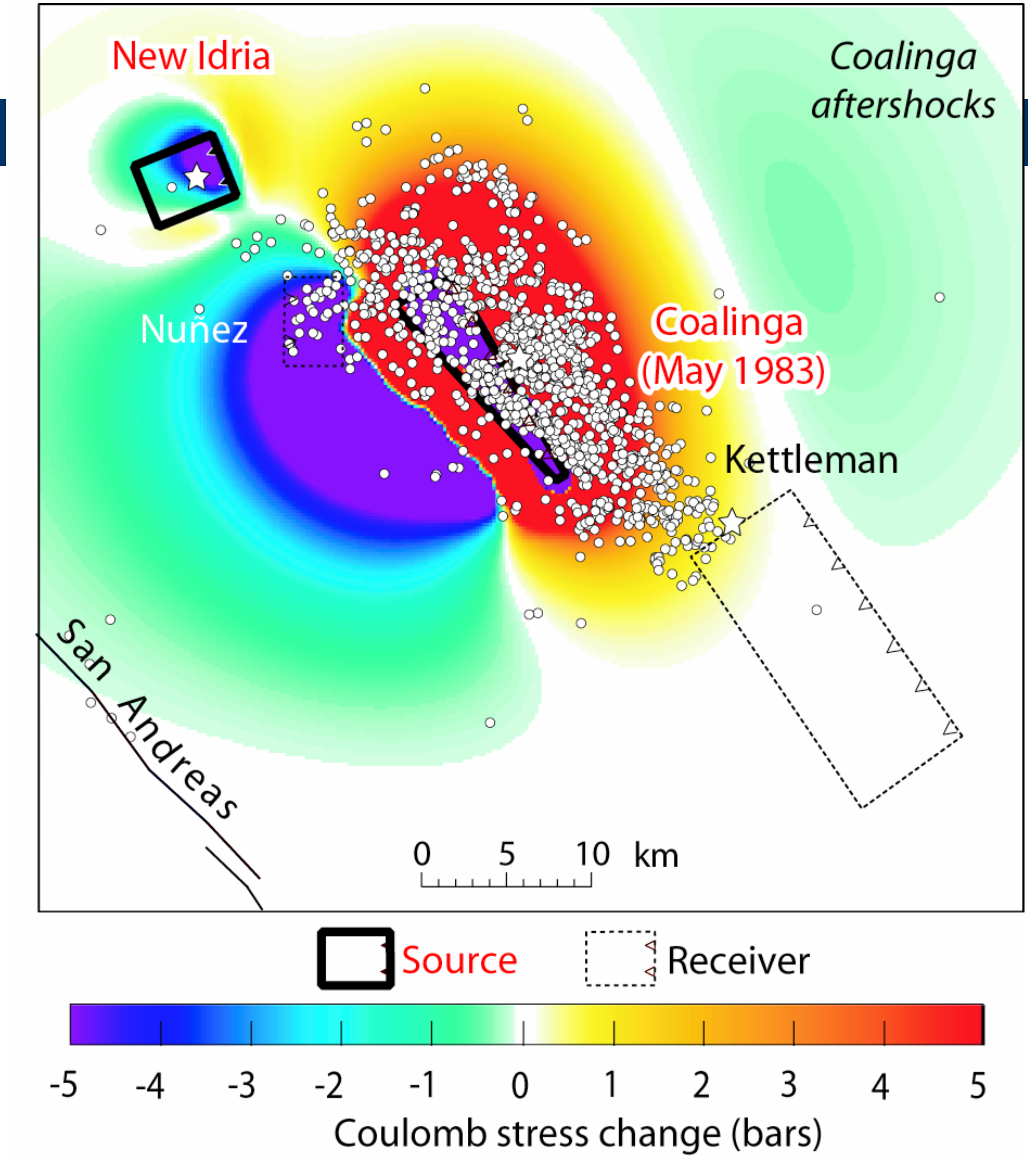

from *Lin & Stein* (JGR, 2004)

Kettleman aftershocks

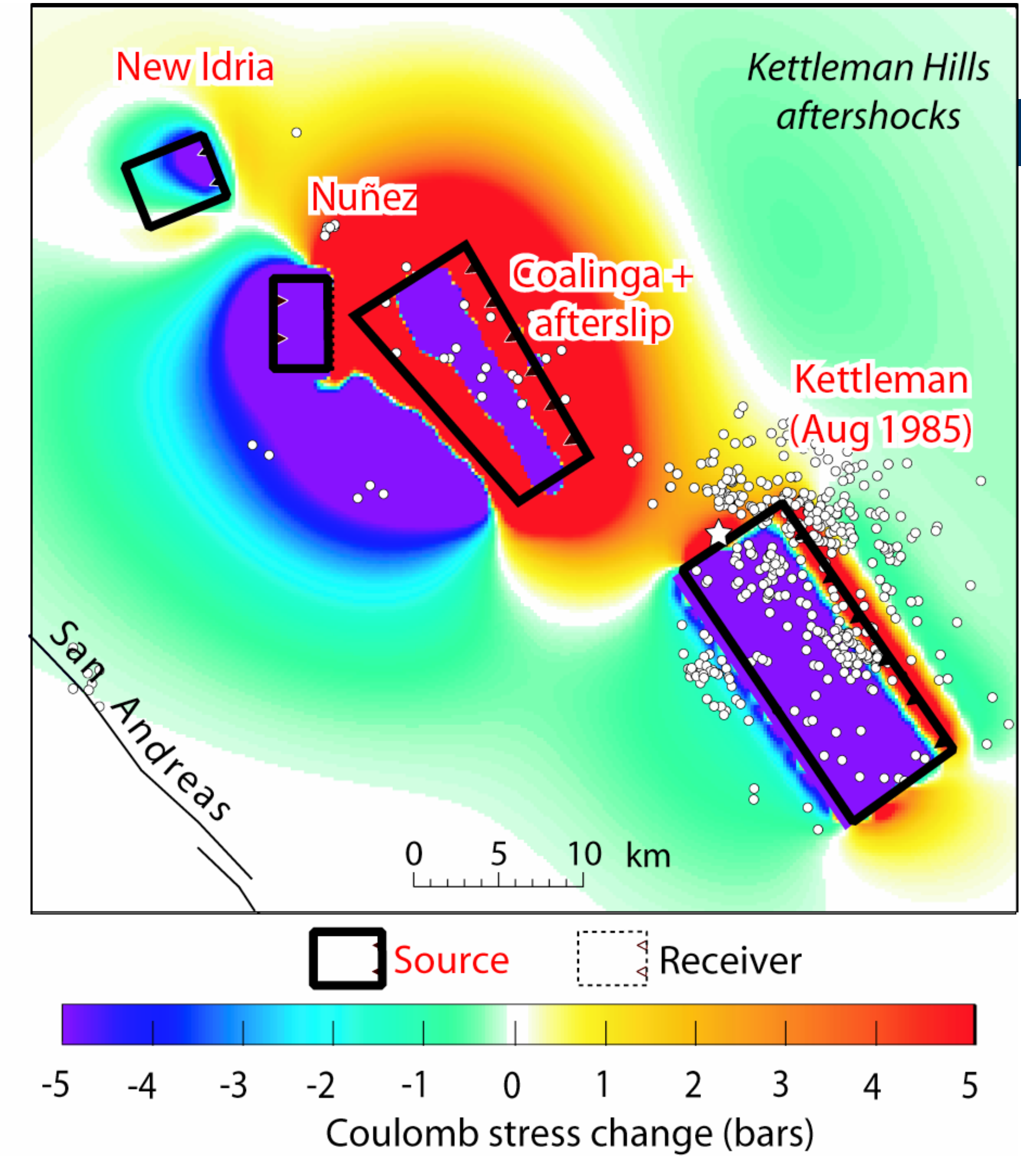

from *Lin & Stein* (JGR, 2004)

Stress Change Correlates with Aftershocks

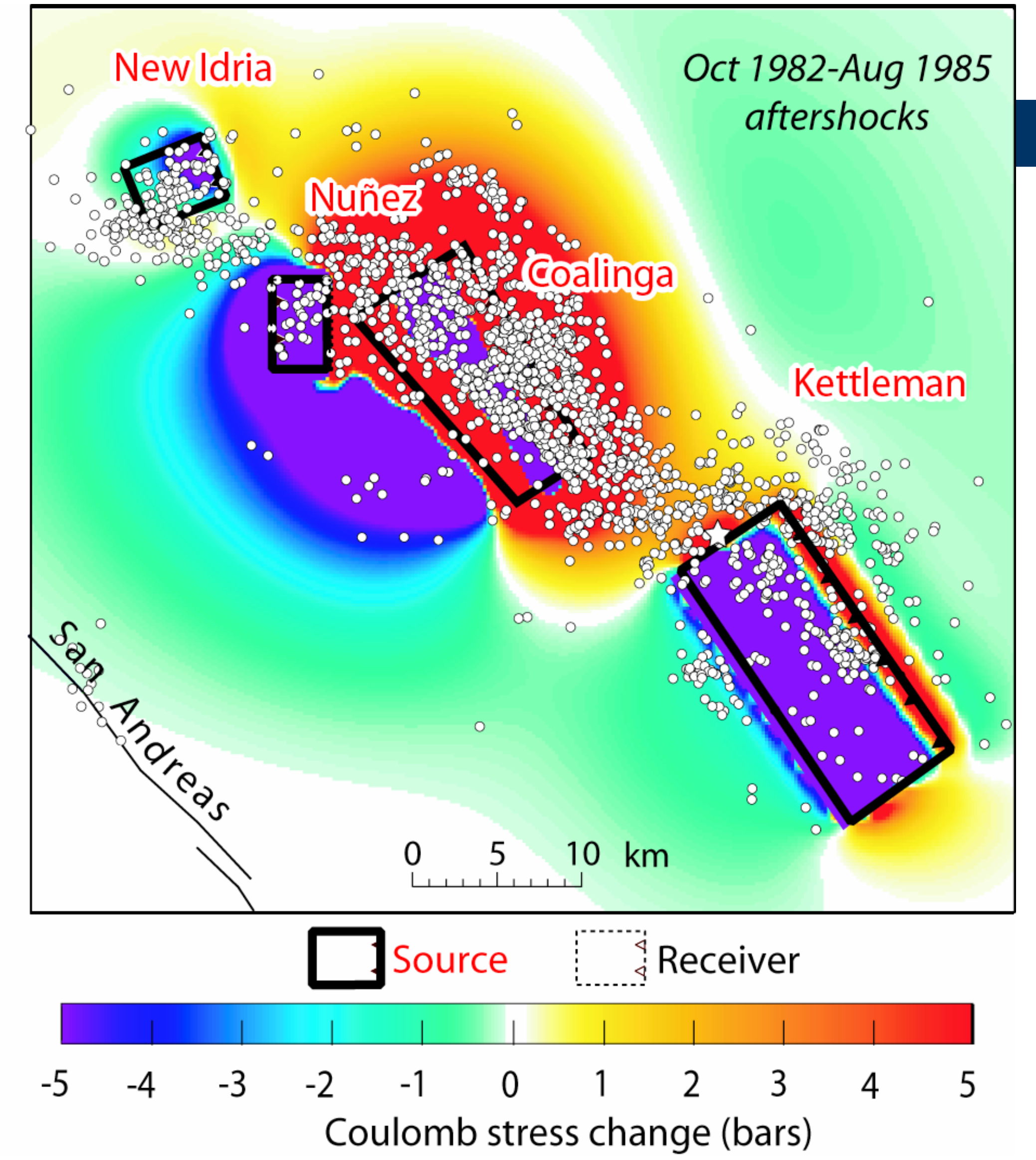

from *Lin & Stein*
(JGR, 2004)

Great 1857 shock stresses northern end of fold belt

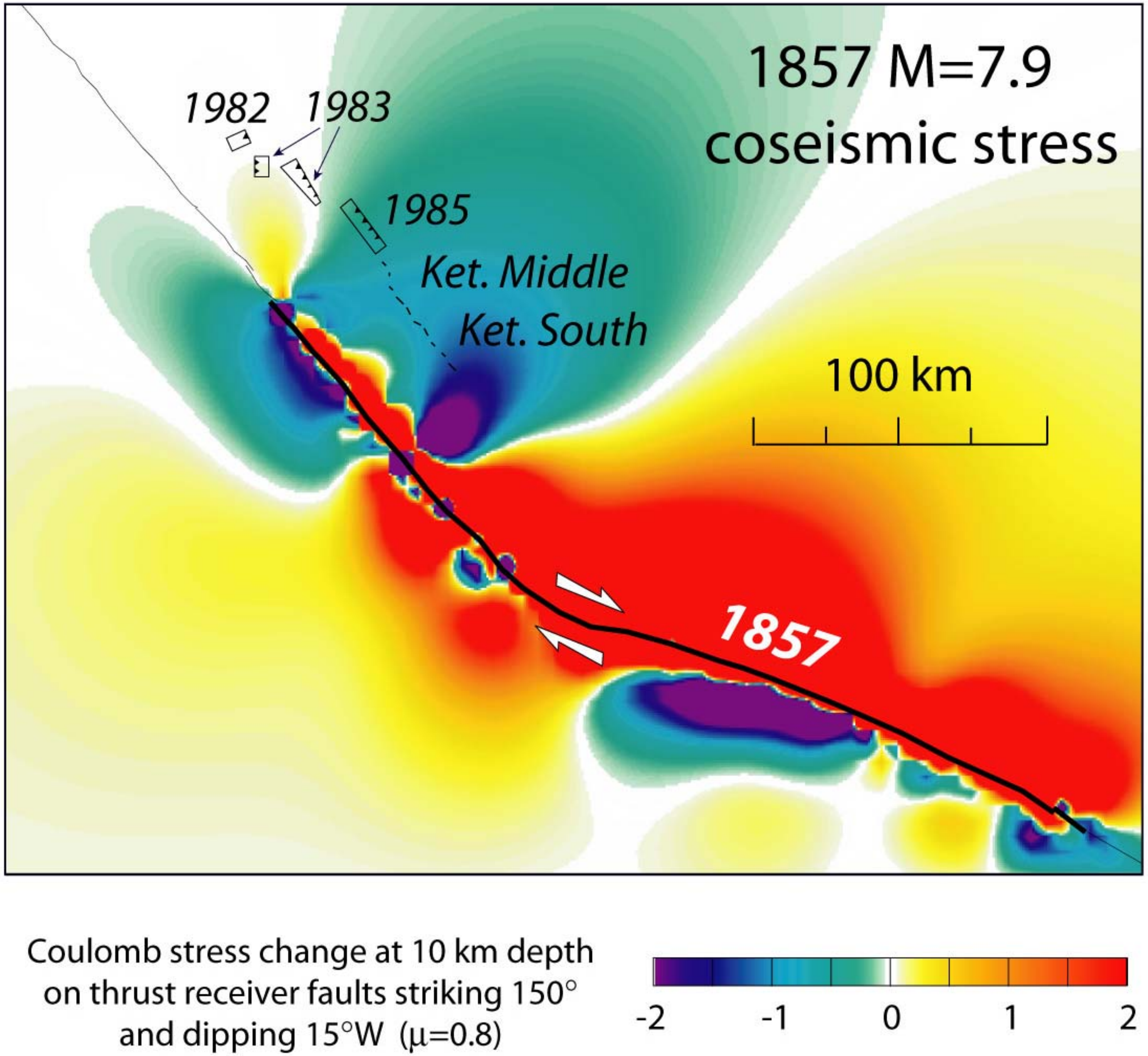

from *Lin & Stein* (JGR, 2004)

ung
005

Combined stresses promote failure on Coalinga folds

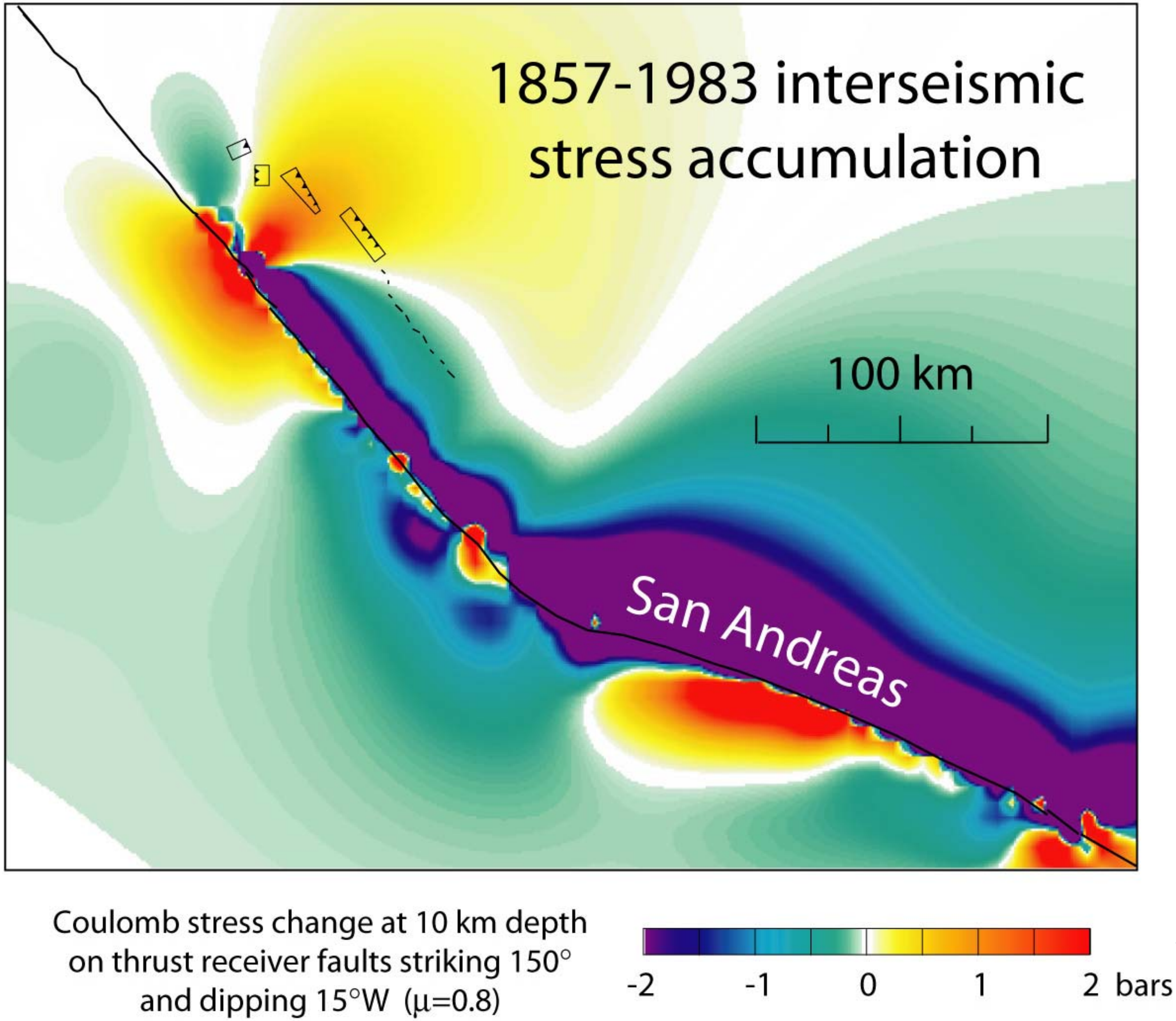

from *Lin & Stein* (JGR, 2004)

The combined stresses Coalinga earthquake sequence

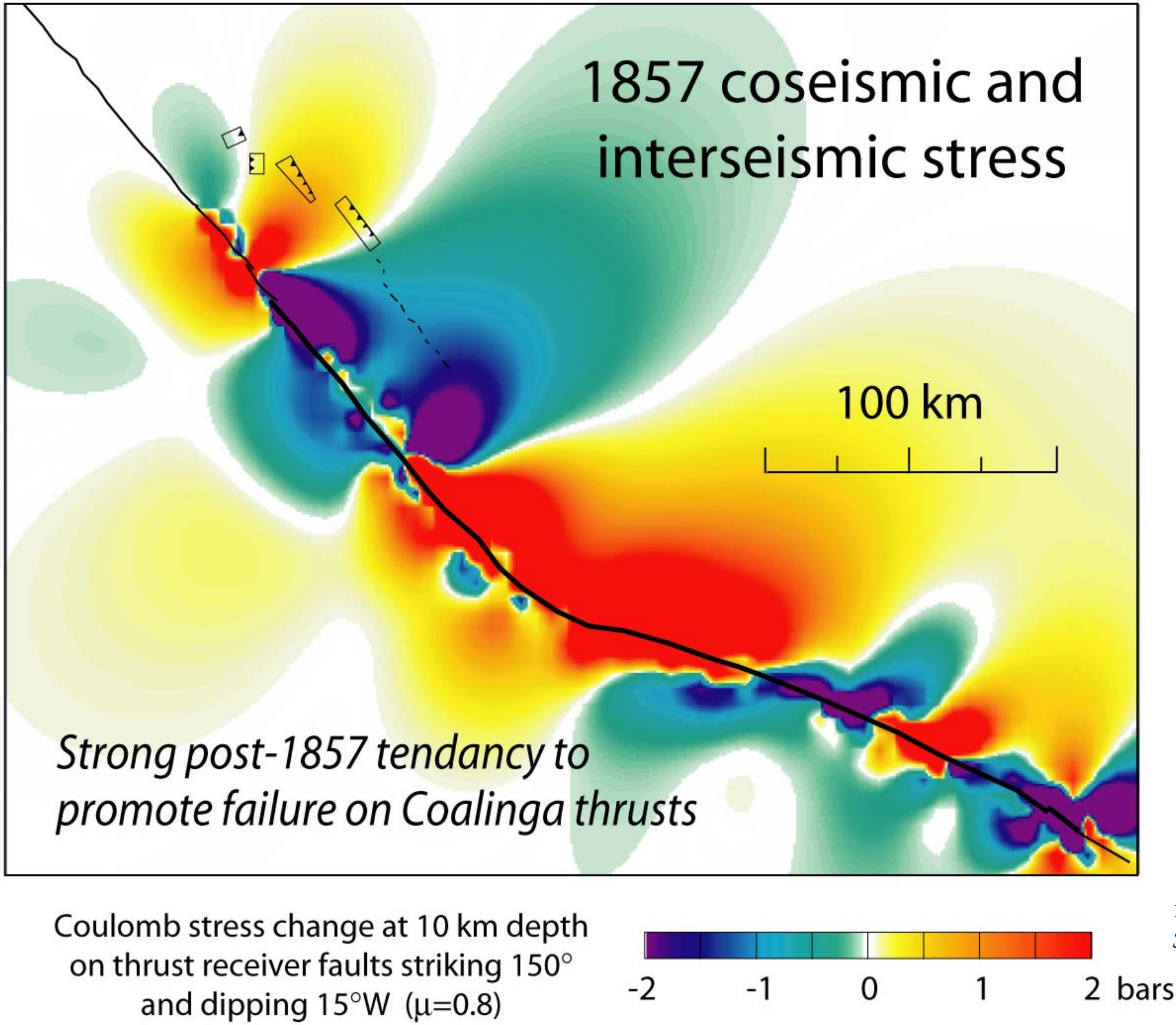

from *Lin & Stein* (JGR, 2004)

Subduction aftershocks and postseismic slip explained by Coulomb stress changes

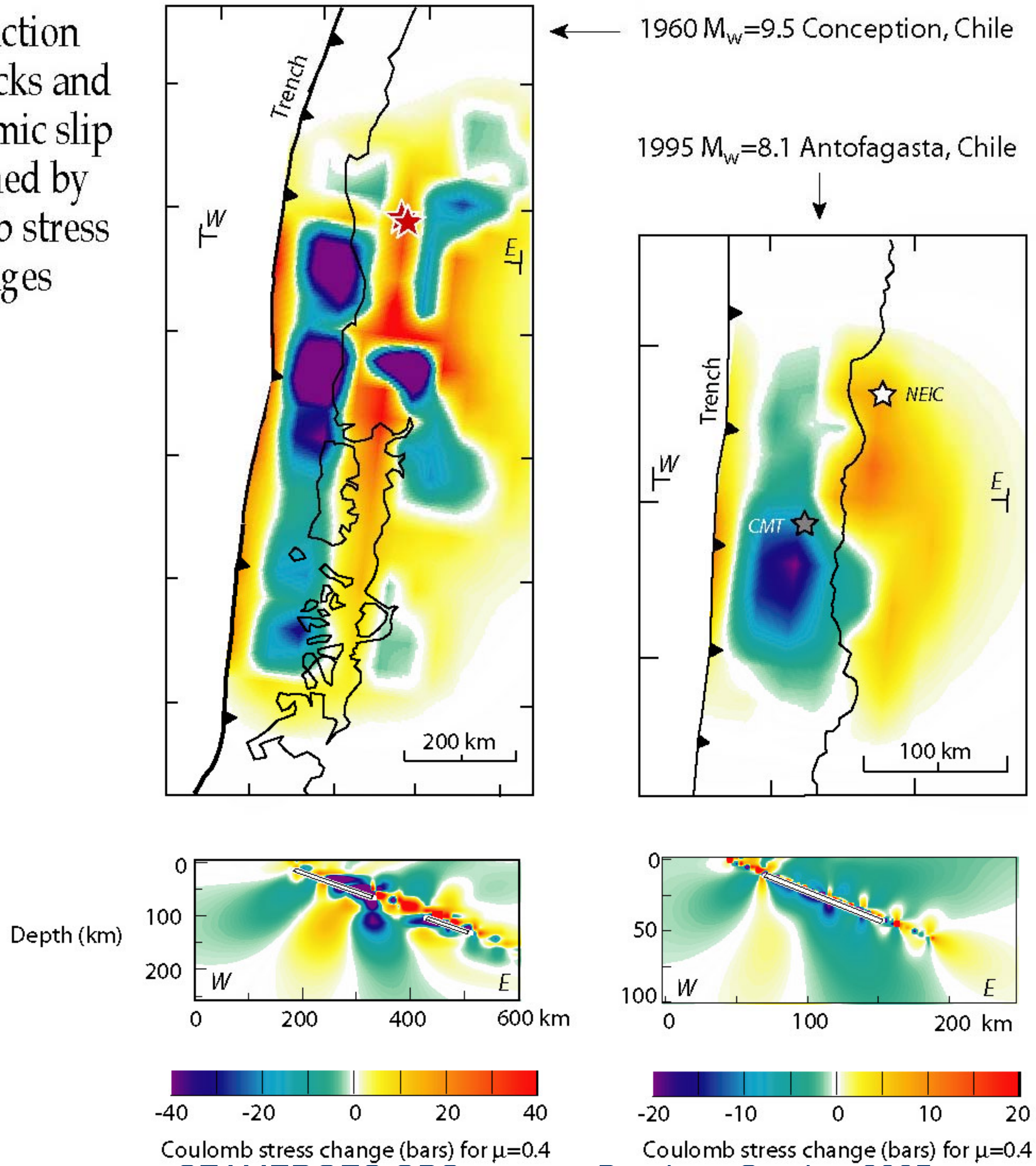

from *Lin & Stein* (JGR, 2004)

Subduction aftershocks and postseismic slip explained by Coulomb stress changes

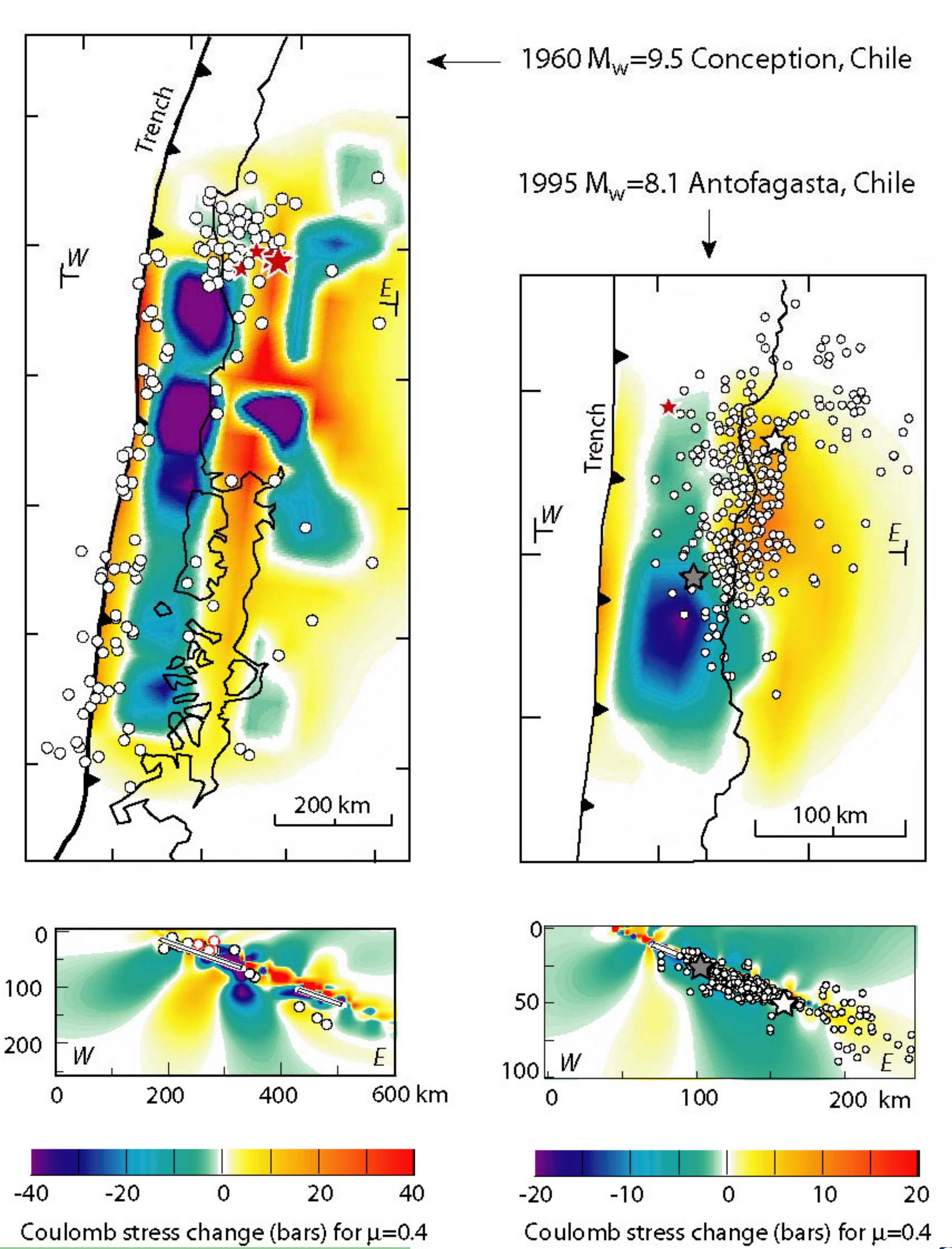

from *Lin & Stein* (JGR, 2004)

Subduction aftershocks and postseismic slip explained by Coulomb stress changes

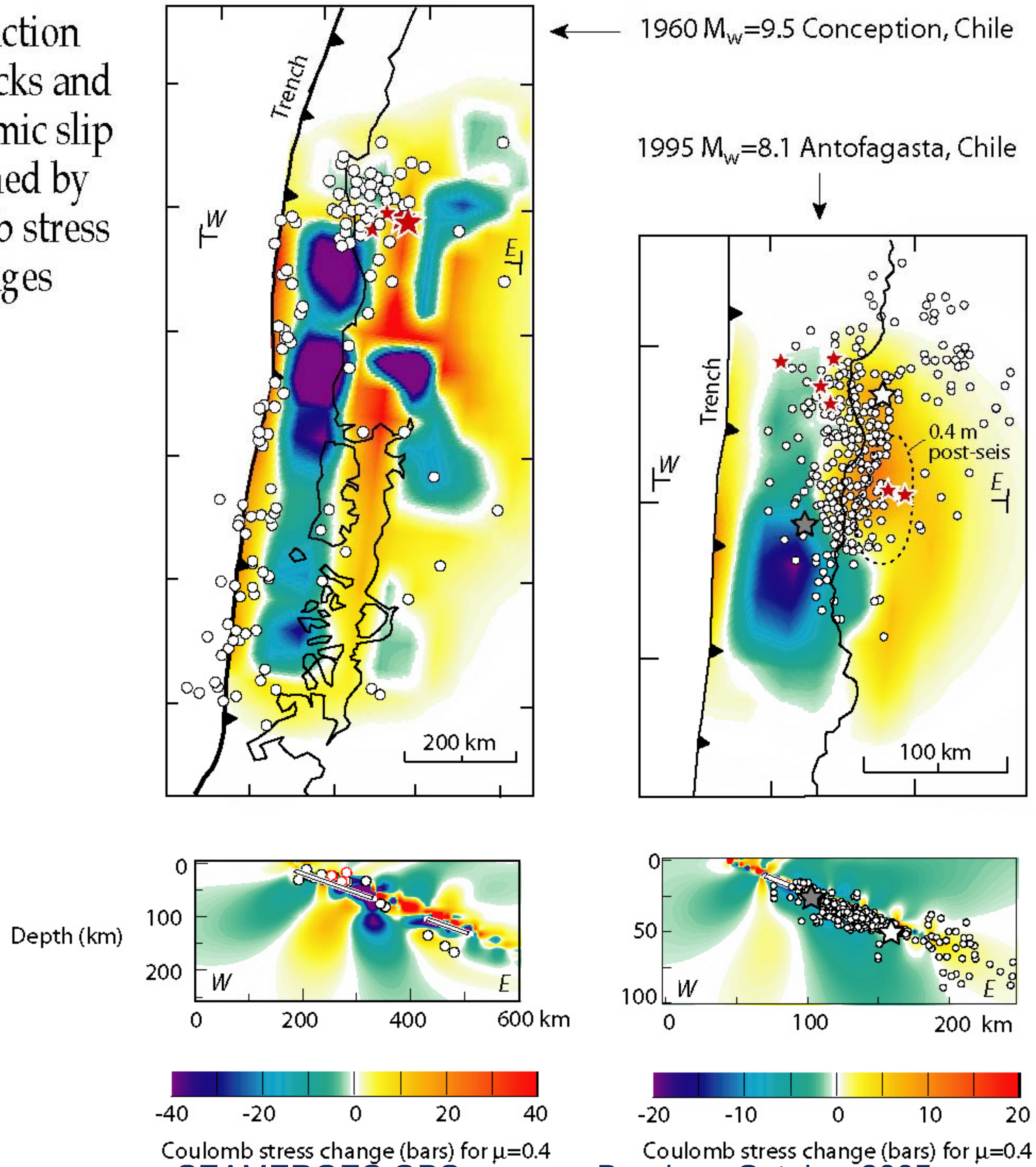

from *Lin & Stein* (JGR, 2004)

Triggering of earthquakes : Vigny et al. JGR 2002

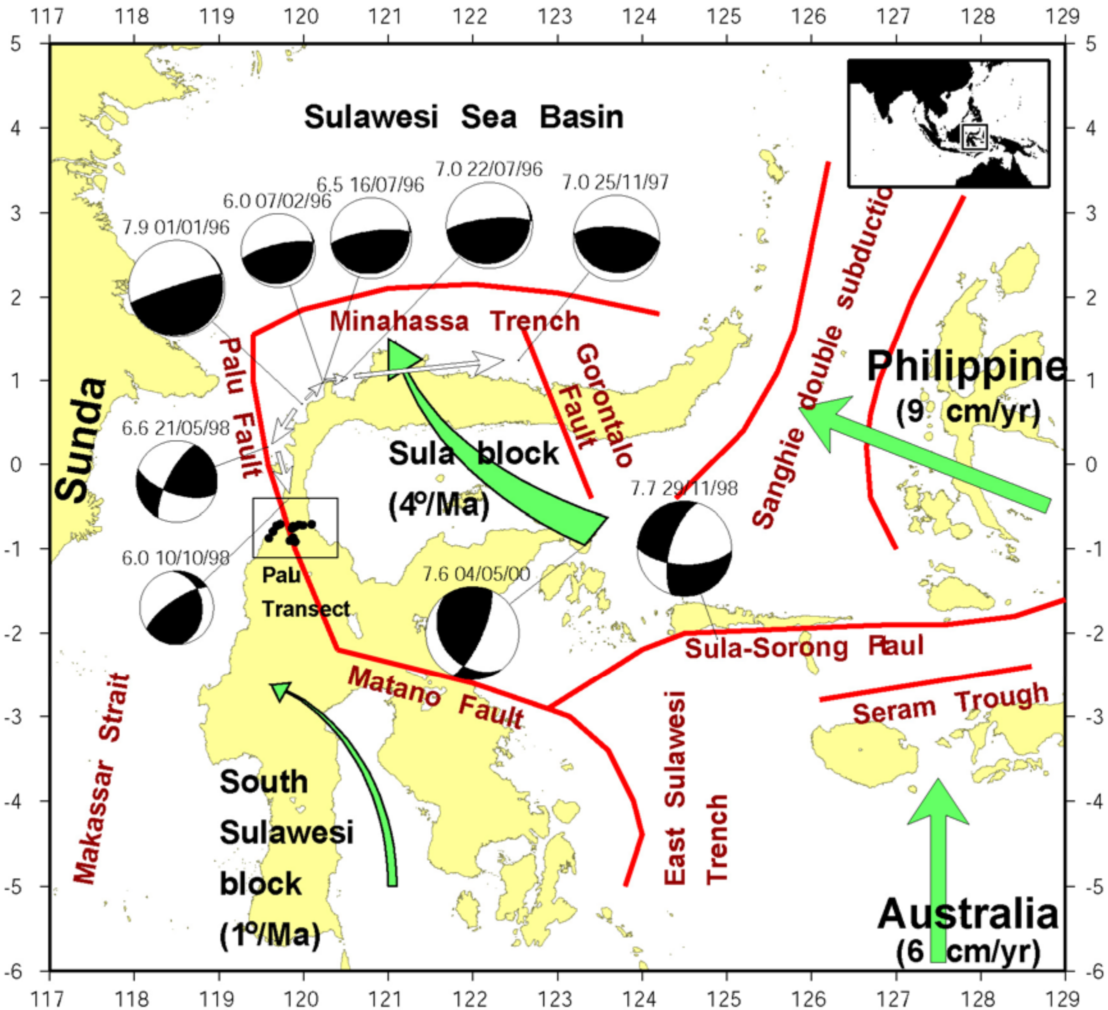

Start :

Mw 7.9 01/01/1996

1st phase :

eastward propagation (2 years) along Minahassa trench

2nd phase :

Southward propagation on Palu fault

3rd phase :

Earthquakes around Sula and Luwuck

Coulomb stress increase

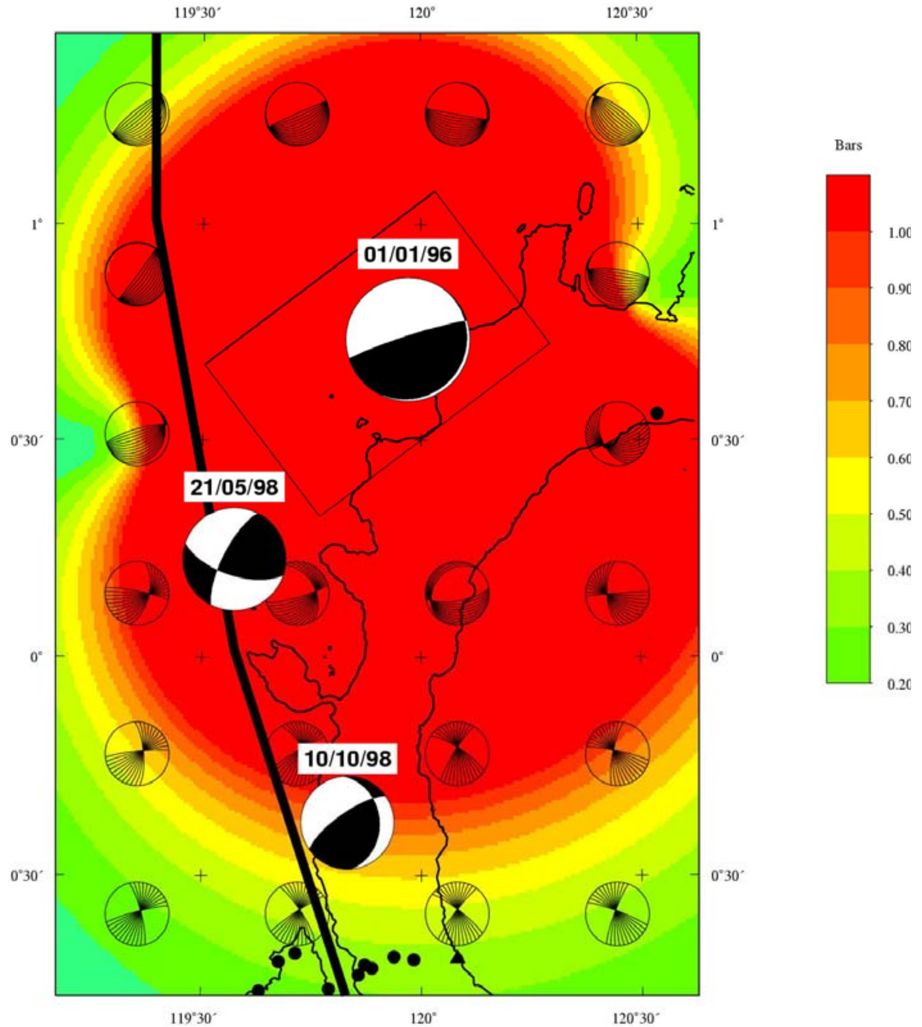

Coulomb Stress generated in North Sulawesi by the 01/01/96 earthquake

Stress is increased by at least 1 bar (red area) almost to Palu

The 2 « Palu fault » earthquakes occur in the area of significant stress increase

Coulomb Stress on Palu fault plane generated by 96 1st Eq

Shear stress on fault plane is increased => slip on fault

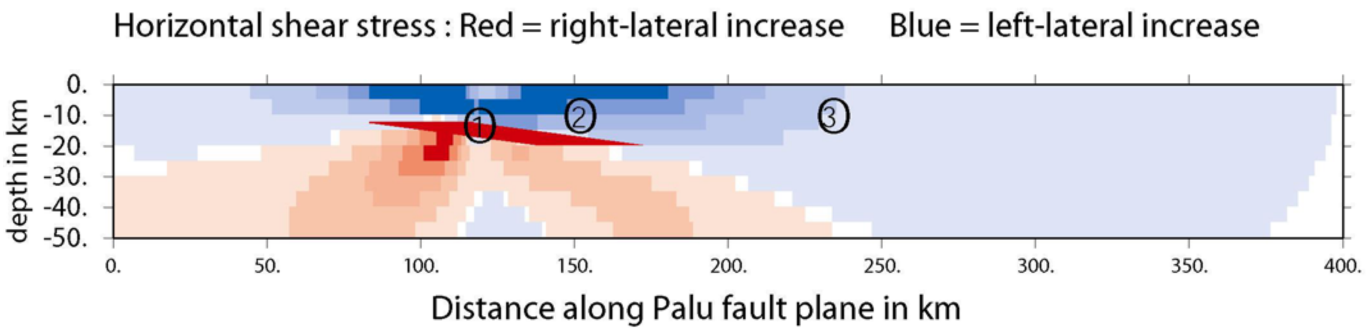

Normal stress on fault is decreased =>unclamping of fault

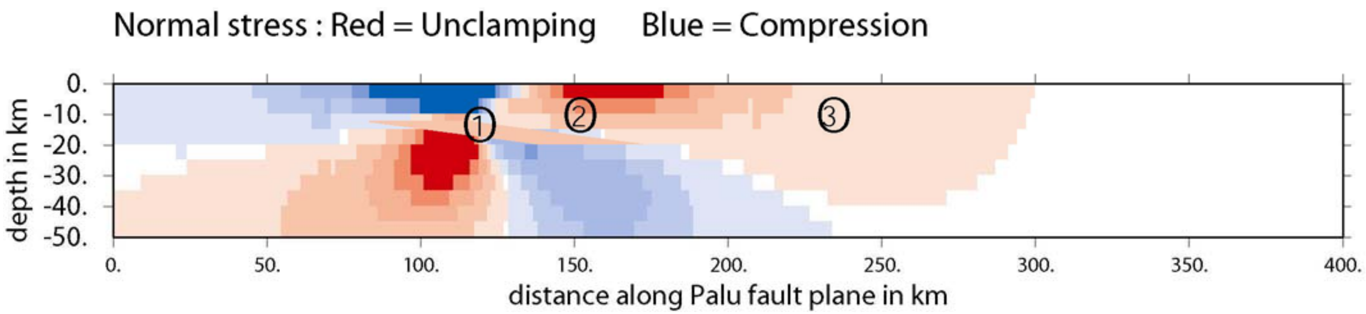

Surface deformation on Palu Transect

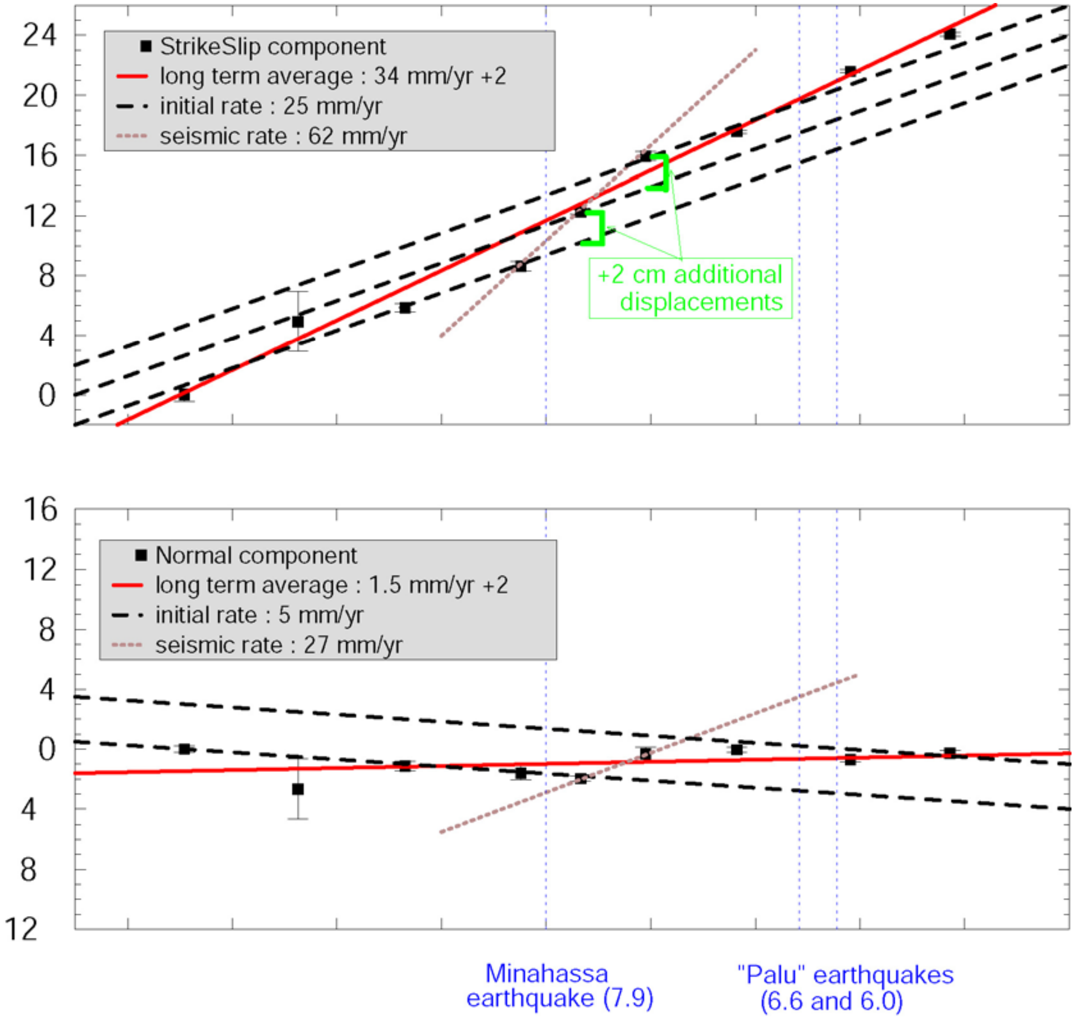

Along strike comp. has been anomalous twice:
- April 96 meas.
- December 96 meas.

The rate is stable since October 97

Normal component has been anomalous :
-December 96
-October 97

The rate is stable since october 98

The 2 earthquakes happened after the rates returned to normal

NAF migration and Marmara sea Coulomb stress increase

Slip.swf

marmara_sea.swf